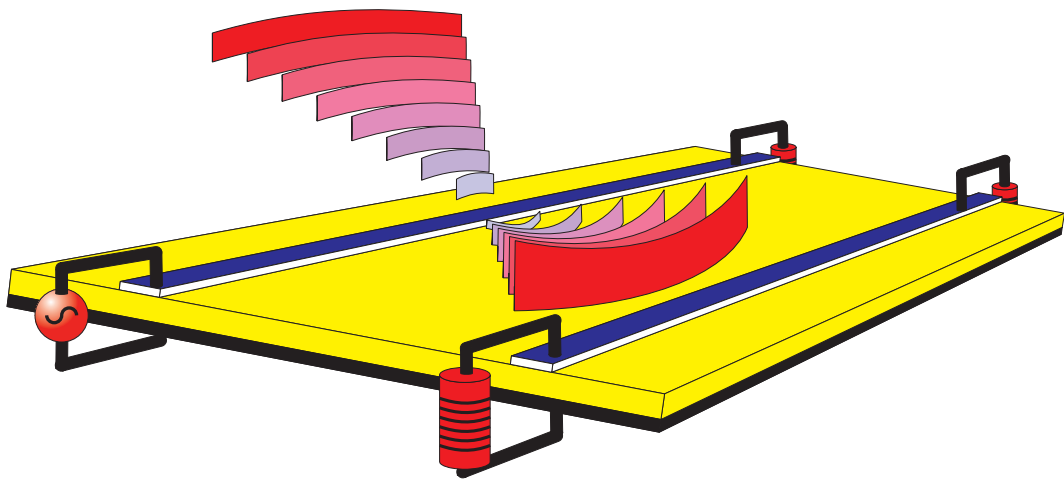


Crosstalk on Printed Circuit Boards

Jan Carlsson

Second Edition



Abstract

This document treats the crosstalk between parallel conductors. The conductors can represent either conductors in a multiconductor cable or traces on a printed circuit board (PCB). An analysis method based on a lumped circuit equivalent for the problem as well as a method to calculate the per unit length parameters are presented. The computed results are validated by comparison with measurements as well as an exact solution of the multiconductor transmission line equations. Several PCB-layouts are analysed to demonstrate how the crosstalk on a PCB can be minimised.

Key words: Crosstalk, Multiconductor transmission line, Mutual coupling, Per unit length parameters.

2nd ed.

**SP Sveriges Provnings- och
Forskningsinstitut**

SP Rapport 1994:14

ISBN 91-7848-721-8

ISSN 0284-5172

Borås 1998

**SP Swedish National Testing and
Research Institute**

SP Report 1994:14

Postal address:

Box 857, S-501 15 BORÅS,

Sweden

Telephone + 46 33 16 50 00

Telex 36252 Testing S

Telefax + 46 33 13 55 02

Contents

	Abstract	2
	Contents	3
	Preface	4
	Summary	5
1	Introduction	7
2	Definition of the problem and general assumptions	8
3	Analysis method	10
3.1	The per unit length parameters	10
3.2	The transmission line equations	12
3.3	Computation of the end-responses	13
4	Validation of computed results	14
4.1	Comparison between the lumped circuit model and the exact solution	14
4.2	Comparison with measurements	18
5	Computed results	22
5.1	General observations for a simple 2-line	22
5.2	Computed results for printed circuit boards	26
5.2.1	Computed results for single layer PCBs	26
5.2.2	Computed results for multilayer PCBs	31
6	Conclusion	38
7	References	39
	Appendix A Determination of the per unit length parameters	40
	Appendix B The computer code LC-Calc	45

Preface

This is the second revised edition of the SP report "Crosstalk on Printed Circuit Boards", originally published 1994. In the second edition the appendix A has been rewritten and the developed computer code, LC-Calc, has been updated to a version running under Windows 95/NT 4.0. Moreover, the program XTalkGen for generation of SPICE files has been included in LC-Calc. Appendix B giving a short description of the LC-Calc program has also been added.

Summary

An efficient and simple method to analyse the crosstalk between adjacent parallel conductors is presented. The method is based on a lumped circuit representation of the multiconductor transmission line and can be applied to conductors in a multiconductor cable as well as traces on a printed circuit board. In order to use the lumped circuit model the per unit length parameters (R, L, C and G) for the multiconductor transmission line have to be known. A finite difference procedure for computing the per unit length parameters L and C, that is suitable for computer implementation, is therefore also presented. One advantage of using the finite difference procedure is that it is easy to analyse configurations with an inhomogenous dielectric, such as for instance a PCB.

The results that are obtained by using the lumped circuit model are shown to have a good agreement with results obtained by measurements. By several examples the effect of using a shielding trace between the generator and the victim trace on a PCB is also shown.

For generating the results in this document a finite difference computer program was developed, LC-Calc. This program computes the L and C-matrices and generates a lumped circuit file that can be used by a circuit analyse program as, for instance, PSPICE. The computer program can be used on an ordinary PC and runs under Windows 95 or NT 4.0 or later. The program is available through the author.

1 Introduction

Many EMC problems on printed circuit boards are caused by the crosstalk, or mutual coupling, between adjacent traces on the board. Therefore, when constructing a printed circuit board, it is important to know how the routing should be done in order to keep the coupling on an acceptable level. It is also important to be able to analyse the coupling before the printed circuit board is manufactured in order to estimate the coupling between different parts.

The crosstalk is a near-field problem and as such often divided into two different parts: common impedance coupling and electromagnetic field coupling. The common impedance coupling is due to the fact that two or several signals share a common return. This part of the crosstalk is the most simple part to analyse and is often the dominating part for low frequencies. The electromagnetic field coupling part of the crosstalk is often divided into inductive and capacitive coupling. The problem when the inductive and capacitive coupling should be analysed is to find the stray inductances and capacitances for the problem.

The techniques discussed in this document can be used for analysing the crosstalk between traces on a printed circuit board as well as between conductors in a multiconductor cable. The analysis is performed in two steps: first the per unit length parameters are calculated and then the responses by using multiconductor transmission line theory.

2 Definition of the problem and general assumptions

The quantity we want to determine is the crosstalk or coupling between adjacent parallel lines. The lines can represent traces on a printed circuit board (PCB) or conductors in a multiconductor cable, see Fig. 2:1. For the case of a PCB the traces could be placed on the top layer of the PCB, as in Fig. 2:1, or be embedded in the dielectric material as for the case of a multilayer board. One or several ground planes can also be present.

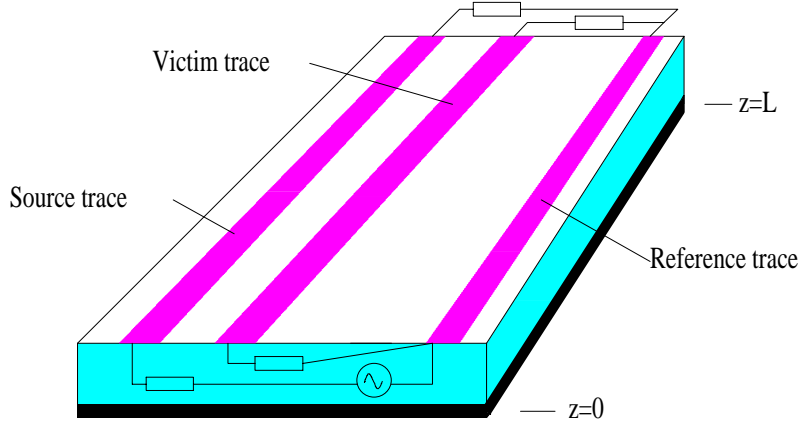


Figure 2:1. Crosstalk between traces on a printed circuit board.

Since we are not interested in the voltages and currents along the lines but only the voltages and currents at the line terminations, the crosstalk can simply be expressed as the ratio of the induced voltage in the victim line to the driving voltage. If a line of the length L is driven at $z=0$, the near-end crosstalk is defined as the ratio of the induced voltage in the victim line at $z=0$ to the driving voltage. The far-end crosstalk for the same line is defined as the ratio of the induced voltage in the victim line at $z=L$ to the driving voltage.

$$\text{We define the crosstalk coefficients as: } \begin{cases} CT_{NE} = \frac{V_{Victim|z=0}}{V_{Source}} \\ CT_{FE} = \frac{V_{Victim|z=L}}{V_{Source}} \end{cases} \quad (2:1)$$

With the knowledge of the crosstalk coefficients we can compute the induced voltage in the victim-line caused by any voltage source on the source-line.

If we assume the lines to be parallel and having the same width along the length and also the cross section to be small compared with the wavelength, the TEM mode will be the only propagating mode on the lines. We can therefore use the transmission line theory to determine the voltages and currents on the lines. Under these assumptions the equivalent circuit for the multiconductor line will be as shown in Fig. 2:2.

We will call the configuration shown in Fig. 2:2 for a N-line. The N-line is defined as a multiconductor line with $N+1$ conductors, including the reference conductor. Thus, for instance, an ordinary two-conductor transmission line (e.g. a coaxial cable) will be a 1-line. The reason for calling the configuration in Fig. 2:2 for a N-line is that we for this configuration can define N unique voltages and N unique currents. We choose to define

the voltages as the potential difference between the lines and the reference line, line 0. All currents are assumed to be returning to the sources through the reference line.

The matrices $[Z_S]$ and $[Z_L]$ represent the source and load impedances respectively. The diagonal elements of these matrices represent the impedances between the lines and the reference conductor and the off-diagonal elements the impedances between different lines.

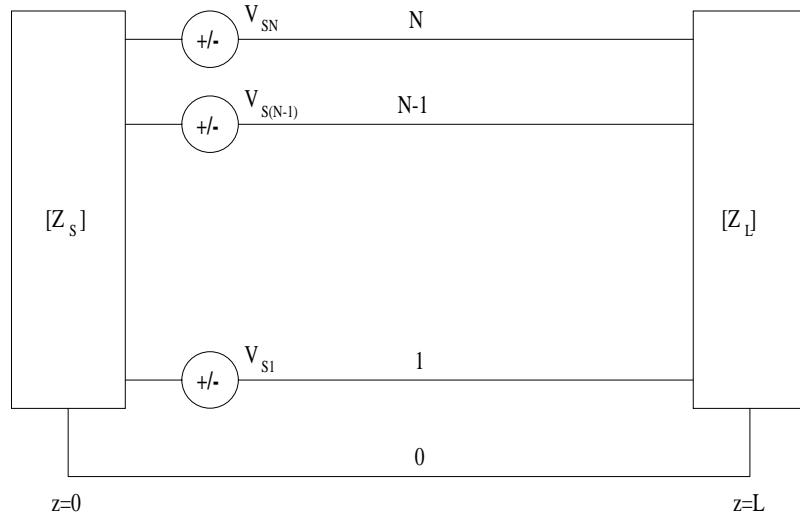


Figure 2.2. Multiconductor transmission line (N-line) excited at $z=0$.

The multiconductor transmission line theory can, in principle, be used for a multiconductor line with an arbitrary number of conductors. However, the number of conductors that can be treated is in practice limited by the computation time required.

As an example the equivalent circuit for the PCB shown in Fig. 2:1 is shown in Fig. 2:3. Note that $Z_{S12} = Z_{S21} = Z_{L12} = Z_{L21} = \infty$ and $V_{S1} = 0$.

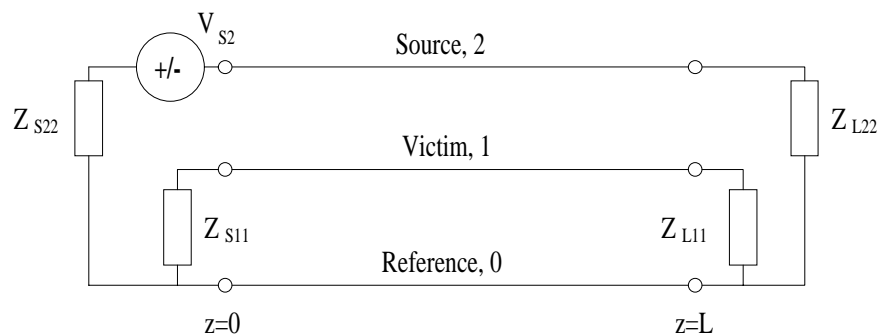


Figure 2.3. Equivalent circuit for the PCB in figure 2:1.

If the lines are not parallel we can, for analysis purposes, approximate the lines as several short sections of parallel lines and apply the transmission line method on these sections, so called staircase approximation.

3 Analysis method

In order to determine the voltages and currents at the terminations of the N-line in Fig. 2:2, several different approaches are possible, either exact (exact in view of the transmission line approximation) or approximate. Furthermore, the analysis can be performed either in the time- or in the frequency-domain. However, a common step in all solution approaches is that we first have to determine the per unit length parameters (R,L,C and G) and then solve for the voltages and currents.

3.1 The per unit length parameters

In order to describe the multiconductor transmission line we use the so called per unit length parameters R,L,C and G (resistance, inductance, capacitance and conductance). For all cases except for the 1-line these parameters are matrices. The diagonal elements in the matrices are associated with self-terms and the off-diagonal elements with mutual terms. As an example a short section of a 2-line and the per unit length matrices are shown in Fig. 3:1.

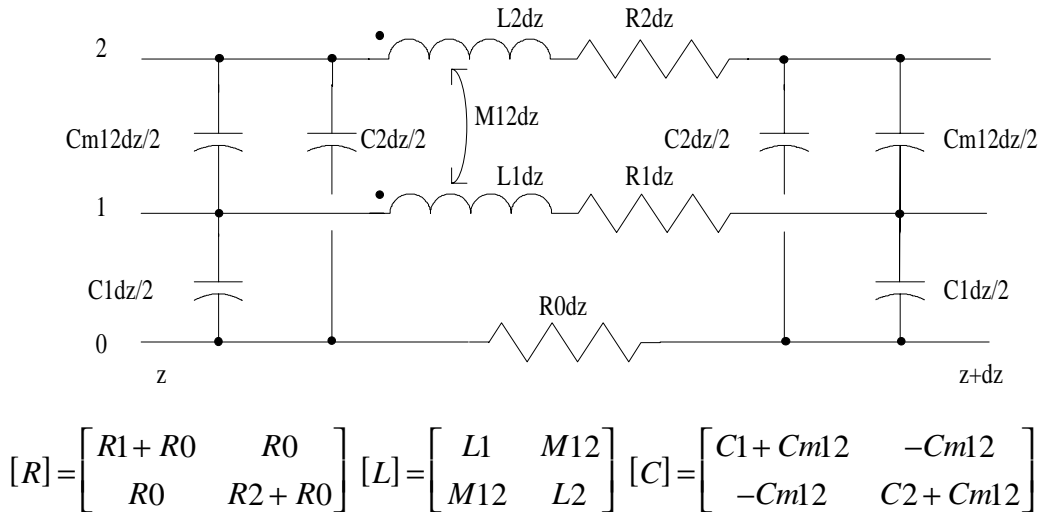


Figure 3:1. Short section of a 2-line (G=0).

The relations between the elements in the per unit length matrices and the individual components in the short lumped section can seem to be strange at first, especially the negative entries in the capacitance matrix. However, if the Kirchoff's voltage and currents laws are applied to the lumped section in Fig. 3:1 and the equations for the voltages and the currents are written in matrix form (equations 3:1 and 3:2), the relations can be understood.

The model for the short section shown in Fig. 3:1 is called a π -section. This model is not the only one possible, other models can be used but the parameters are the same.

For lossless lines the resistance, R, and the conductance, G, are both equal to zero. The assumption of a lossless line is very often used and is usually a very good approximation for real cases. If losses should be taken into account this is usually done by assuming some resistance and still letting the conductance be equal to zero. The resistance for the conductors are in general frequency dependent, through the skin depth, but the DC-approximation often provides a sufficient accuracy. The resistance, R, represents losses in

the conductors while the conductance, G , represents losses in the medium between the conductors (dielectric losses).

The assumed TEM mode in the multiconductor transmission line has a field pattern that looks the same as the electrostatic field pattern. We can therefore determine the per unit length capacitances and inductances by solving the electrostatic case. The field distribution for the electrostatic case satisfies the Laplace equation in two-dimensions, which accordingly has to be solved. In order to solve the Laplace equation the choice in this document is to use an iterative finite difference procedure, see appendix A.

For a N -line the capacitance matrix will be of dimension N by N . For the example shown in Fig. 3:2 the capacitance matrix is of dimension 5 by 5.

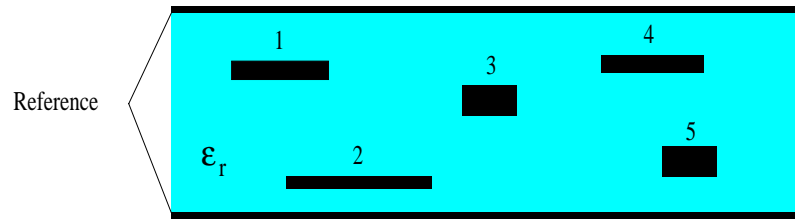


Figure 3:2. Cross section of a N -line ($N=5$).

The capacitance matrix is a symmetric matrix because $C_{ij} = C_{ji}$. The elements in the capacitance matrix satisfy the following relations:

$$\begin{cases} C_{ii} \geq 0 \\ C_{ij} \leq 0 \text{ for } i \neq j \\ C_{ij} = C_{ji} \end{cases}$$

The ij -element in the capacitance matrix can be determined as, [1]: $C_{ij} = \frac{Q_i}{V_j} \Big|_{V_m=0, m \neq j}$, i.e.

the ij -element is equal to the ratio of the charge on conductor i caused by the voltage on conductor j to the voltage on conductor j . Thus, in order to determine the capacitance matrix for a N -line, we have to solve the Laplace equation for the configuration N -times with different boundary conditions.

The solution of the Laplace equation gives the potential distribution in the region and we can, by applying Gauss' law, determine the charge per unit length on conductor i as:

$$Q_i = -\oint_{l_i} \epsilon \nabla V \cdot \hat{n} dl_i \text{ where } l_i \text{ is a closed line around conductor } i, \hat{n} \text{ is an outward}$$

directed unit vector and V is the potential distribution.

The inductance matrix can be computed by the knowledge of the capacitance matrix for the case when all material in the cross section is free space, i.e. [2]: $[L] = \mu_0 \epsilon_0 [C_0]^{-1}$ where $[C_0]$ is the capacitance matrix when all dielectric material in the cross section is replaced by free space.

The strategy for computing the per unit length capacitances and inductances discussed above was incorporated in a computer program that can be used on an ordinary PC. The computer program solves the Laplace equation by an iterative finite difference method and, when this is done, integrates around the conductor in order to compute the enclosed

charge, and thereby the capacitance. Finally the inductance matrix is computed by inverting the free space capacitance matrix. The details of how the program works can be found in appendix A.

3.2 The transmission line equations

The equations for the voltages and currents on a multiconductor transmission line can be obtained by simply replacing the scalar quantities in the ordinary transmission line equations (for the 1-line) with the corresponding vector quantities. Also the impedances R,L,C and G have to be replaced with the corresponding matrix expressions. The equations, in the time-domain, will then be:

$$\begin{cases} \frac{\partial}{\partial z}[V] = -[R][I] - [L]\frac{\partial}{\partial t}[I] \\ \frac{\partial}{\partial z}[I] = -[G][V] - [C]\frac{\partial}{\partial t}[V] \end{cases} \quad (3:1)$$

and in the frequency-domain:

$$\begin{cases} \frac{d}{dz}[V] = -[Z][I] \\ \frac{d}{dz}[I] = -[Y][V] \end{cases} \quad \text{where} \quad \begin{cases} [Z] = [R] + j\omega[L] \\ [Y] = [G] + j\omega[C] \end{cases} \quad (3:2)$$

The multiconductor transmission line equations (3:1) and (3:2) can be solved exactly, see for instance [3] and [4]. The solution for the currents, in the frequency-domain, can be expressed as, [3, Sec. 1.3.2.2]:

$$\begin{bmatrix} [I(0)] \\ [I(L)] \end{bmatrix} = \begin{bmatrix} [[\delta] + [\Gamma_1]] & [0] \\ [0] & [[\delta] + [\Gamma_2]] \end{bmatrix} \begin{bmatrix} [-\Gamma_1] & [T]e^{[\gamma]L}[T]^{-1} \\ [T]e^{[\gamma]L}[T]^{-1} & [-\Gamma_2] \end{bmatrix}^{-1} \begin{bmatrix} [\alpha_1] \\ [\alpha_2] \end{bmatrix} \quad (3:3)$$

where:

$$[I(0)] = \begin{bmatrix} I_1(z=0) \\ I_2(z=0) \\ \dots \\ I_N(z=0) \end{bmatrix}, \quad [\delta] = \begin{bmatrix} 1 & 0 & \dots & 0 \\ 0 & 1 & \dots & \dots \\ \dots & \dots & \dots & \dots \\ 0 & \dots & \dots & 1 \end{bmatrix}, \quad [\Gamma_1] = [[Z_s] + [Z_c]]^{-1}[[Z_s] - [Z_c]]$$

$$[\Gamma_2] = [[Z_L] + [Z_c]]^{-1}[[Z_L] - [Z_c]], \quad [Z_c] = [Y]^{-1}[T][\gamma][T]^{-1} \quad (3:4)$$

$$[T]^{-1}[Y][Z][T] = [\gamma]^2, \quad [\alpha_1] = \frac{1}{2}[Z_c]^{-1}[V_s], \quad [\alpha_2] = \frac{1}{2}[T]e^{[\gamma]L}[T]^{-1}[Z_c]^{-1}[V_s]$$

and the corresponding voltages as:

$$\begin{aligned} [V(0)] &= -[Z_s][I(0)] \\ [V(L)] &= [Z_L][I(L)] \end{aligned} \quad (3:5)$$

In the expressions the matrix $[V_s]$ represents the exciting voltage sources at $z=0$, the matrix $[T]$ is a transformation matrix consisting of the eigenvectors of the matrix $[Y][Z]$ and the $[\gamma]^2$ matrix is a diagonal matrix with elements equal to the corresponding eigenvalues.

In the general case, the main difficulty in using equation (3:3) is to find the transformation matrix $[T]$ and the eigenvalues $[\gamma]^2$. This can be a difficult task since the matrix $[Y][Z]$ is not, in general, a symmetric matrix. However, for the homogeneous and lossless case the transformation matrix will be the unit matrix and the eigenvalues will correspond to the velocity of propagation on the line, i.e. $[\gamma] = j\omega\sqrt{\mu\epsilon}[1]$.

Another, and perhaps more intuitive, way to solve the equations (3:1) and (3:2) is to use the lumped-circuit model for the line. In this model, which is an approximate model, the line is divided into a number of small sections each of which is characterised by the per unit length parameters. Several different models for the small sections are possible, the one shown in Fig. 3:1 is known as the π -section model.

When we use the lumped circuit model it is important to realise the difference between the component values in the model and the entries in the per unit length matrices. By comparing the definition of the per unit length matrices with the lumped circuit model we can define the following relations, see Fig. 3:1:

$$\begin{cases} R_{ij} = R_0, & i \neq j \\ R_{ii} = R_i + R_0 \end{cases} \quad \begin{cases} L_{ij} = M_{ij}, & i \neq j \\ L_{ii} = L_i \end{cases} \quad \begin{cases} C_{ij} = -C_{mij}, & i \neq j \\ C_{ii} = C_i + \sum_{j \neq i} C_{mij} \end{cases} \quad (3:6)$$

where the left-hand sides represent the entries in the matrices, the right-hand sides the components in the circuit model and $M_{ij} = M_{ji}$, $C_{mij} = C_{mji}$.

The lumped circuit model is simple to use and the responses can conveniently be computed, either in the time- or in the frequency-domain, with an ordinary circuit simulator as, for instance, SPICE.

3.3 Computation of the end-responses

The method to compute the end-responses or the crosstalk coefficients, as defined in equation (2:1), that is used in this document is as follows:

First, the per unit length matrices $[R]$, $[L]$ and $[C]$ are computed by using the technique that is described in appendix A. The developed computer code, LC-Calc, can also create a circuit file containing an arbitrary number (chosen by the user) of lumped circuit sections. Finally, the circuit file is used in PSPICE where the lines can arbitrary be loaded and the analysis can be performed either in the time- or in the frequency-domain.

4 Validation of computed results

4.1 Comparison between the lumped circuit model and the exact solution

In order to determine how well the lumped circuit model can predict the end-responses of a multiconductor transmission line, a comparison with the exact solution for a simple example was done. The exact solution was computed using equation (3:3) and the example multiconductor line is shown in Fig. 4:1. Two different load cases were considered:

$$1: \begin{cases} R_{S11} = 50 \\ R_{L11} = 50 \\ R_{L22} = 50 \end{cases} \quad 2: \begin{cases} R_{S11} = 1000 \\ R_{L11} = 1000 \\ R_{L22} = 1000 \end{cases}$$

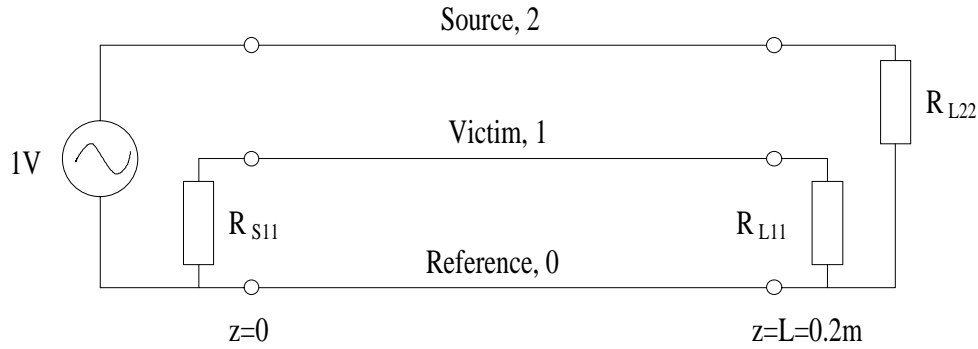


Figure 4:1. 2-Line used for comparison between lumped circuit model and exact solution.

The treated 2-line is only a fictive line and the per unit length parameters are chosen to be (see eq. (3:6) and Fig. 3:1):

$$[L] = \begin{bmatrix} 0.5 & 0.15 \\ 0.15 & 0.5 \end{bmatrix} \mu\text{H} / \text{m} ; [C] = \begin{bmatrix} 24.4 & -7.3 \\ -7.3 & 24.4 \end{bmatrix} \text{pF} / \text{m}$$

$$L_1 = L_2 = 0.5 \mu\text{H} / \text{m} ; M_{12} = 0.15 \mu\text{H} / \text{m} ; C_1 = C_2 = 17.1 \text{pF} / \text{m} ; C_{m12} = 7.3 \text{pF} / \text{m}$$

The propagation velocities on the lines are that of free space and the lengths of the lines are 0.2 m. This gives that the length of the line is one wavelength at 1.5 GHz.

The following circuit file for the 1-section lumped model and load case 1 was used as input file for PSPICE:

```

* Lumped circuit representation of a MTL

* Input nodes of the MTL:
*   Reference: Node 0
*   Line 1   : Node 1
*   Line 2   : Node 2

* Output nodes of the MTL:
*   Reference: Node 5
*   Line 1   : Node 6
*   Line 2   : Node 7

* Lumped section number 1
C0 1 0 1.71E-0012
C1 2 0 1.71E-0012
C2 2 1 7.30E-0013

L1 1 3 1.00E-0007
L2 2 4 1.00E-0007

K0 L1 L2 3.00E-0001

R0 0 5 1.00E-0010 *Resistance may not be zero
R1 3 6 1.00E-0010
R2 4 7 1.00E-0010

C3 6 5 1.71E-0012
C4 7 5 1.71E-0012
C5 7 6 7.30E-0013

* Load case 1
VIN 2 0 AC 1
RS11 1 0 50
RL11 6 5 50
RL22 7 5 50

.AC OCT 20 100K 1G
.PRINT AC V(1) V(6,5) *Near- and far-end responses
.END

```

The computed responses were the crosstalk coefficients, as defined in equation (2:1), and the results are shown in Fig. 4:2-4:5. As seen from the results the agreement between the lumped circuit model and the exact solution is excellent up to 1 GHz when only five lumped sections are used (the line length is equal to $2/3\lambda$ and each lumped section $\approx 0.13\lambda$). When one lumped section is used the agreement is good up to about 200 MHz (the length of the lumped section is $\approx 0.13\lambda$). The conclusion is that each section in the lumped circuit model should not be longer than about one tenth of the wavelength on the line.

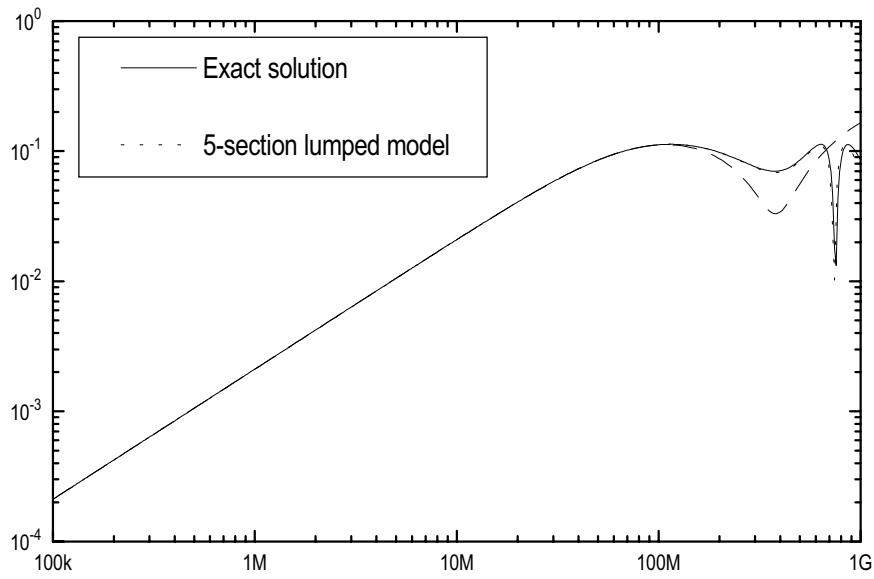


Figure 4.2. Near-end crosstalk coefficient for load case 1.

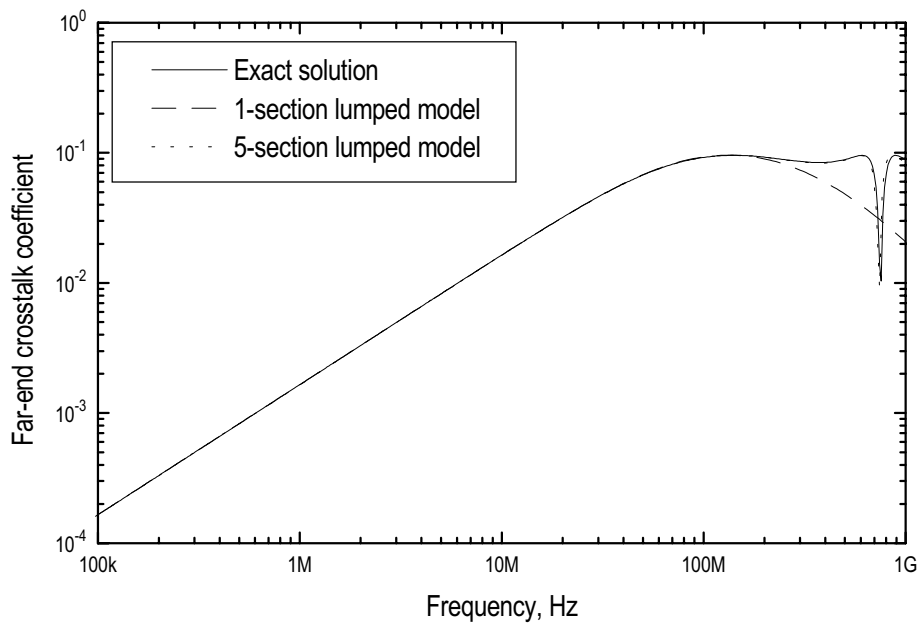


Figure 4.3. Far-end crosstalk coefficient for load case 1.

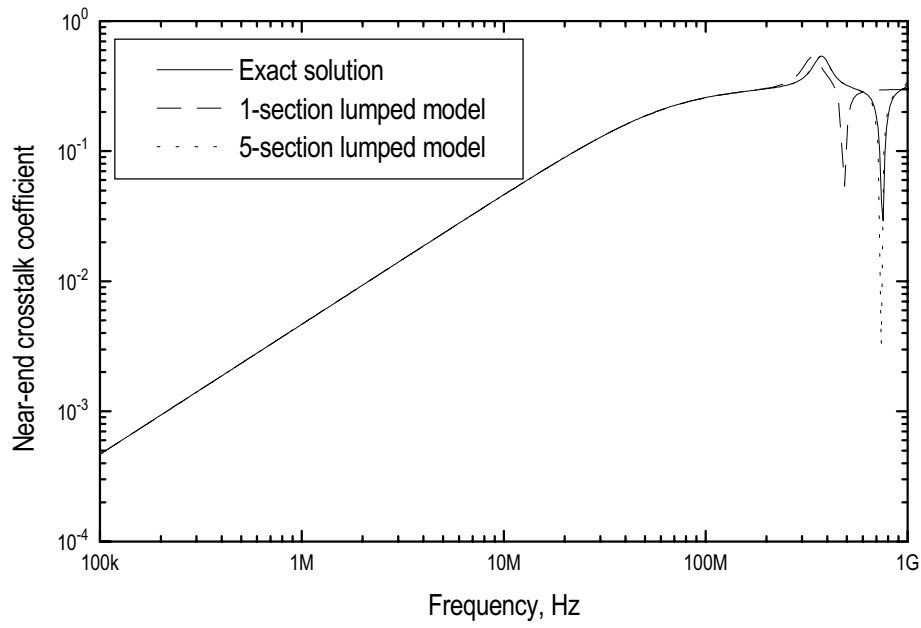


Figure 4.4. Near-end crosstalk coefficient for load case 2.

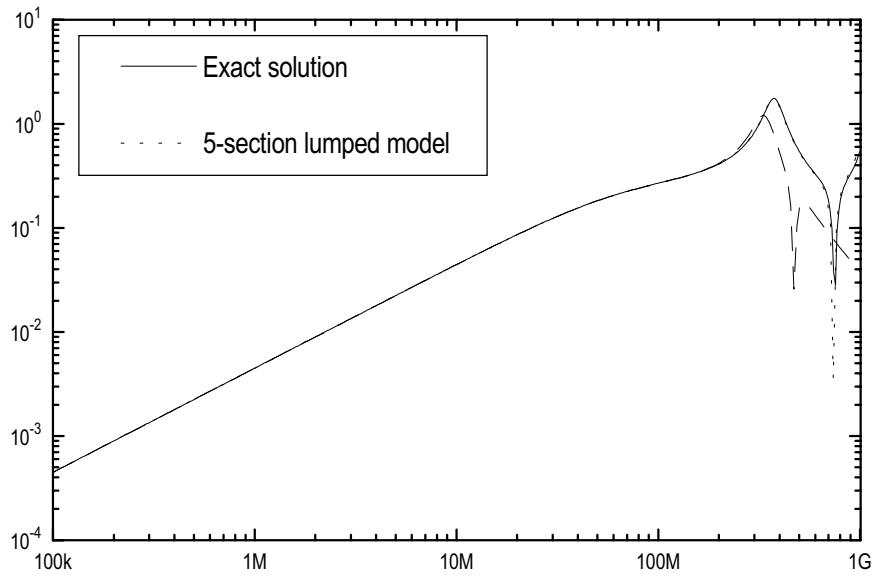


Figure 4.5. Far-end crosstalk coefficient for load case 2.

4.2 Comparison with measurements

In order to validate the computed results, a comparison with measurements on a simple PCB was performed. The PCB was a glass-epoxy ($\epsilon_r = 4.7$) board with a copper plane on one side and two parallel traces on the other side, the configuration is shown in Fig. 4:6.

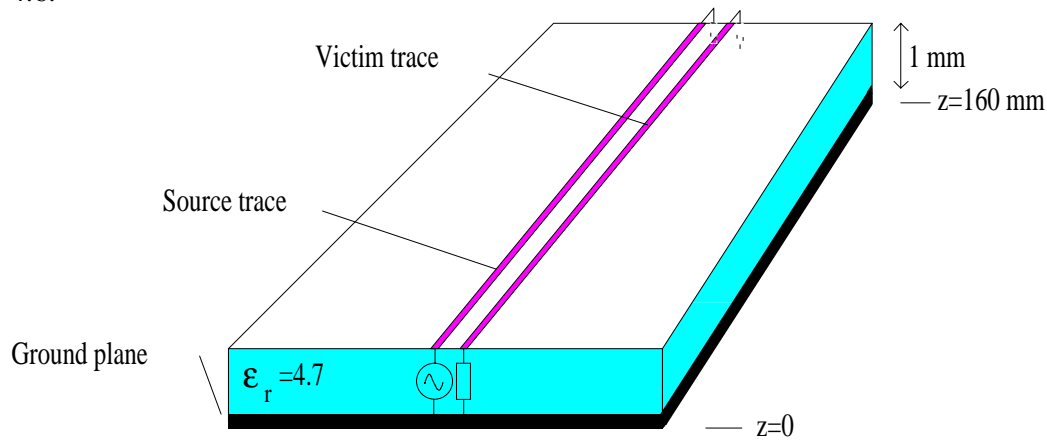


Figure 4:6. PCB used for measurements. Both traces are 2.2 mm wide and the centre to centre distance is 4.0 mm.

One of the traces was excited at one end and terminated with a 1 kOhm resistor at the other end. The second trace was terminated with 1 kOhm resistors at both ends. Measurements and computations were performed in the time domain as well as in the frequency domain. The computation was performed as described in chapter 3.3 and three lumped sections were used for describing the 2-line.

The excitation voltage waveform for the time domain experiment is shown in Fig. 4:7 and the measured and computed results are shown in Fig. 4:8 and 4:9 respectively. As seen from the results the agreement is fairly good and the deviation between measured and computed results can be explained by not knowing the various parameters (dielectric constant etc.) exactly and also by measurements uncertainty. However, the shape of the waveform is predicted very well and this was also confirmed with other types of excitation waveforms (square wave etc.).

The results for the frequency domain experiment are shown in Fig. 4:10 and also for this case the agreement is good.

In order to compute the per unit length parameters, the program LC-Calc was used. For the computation with LC-Calc the following parameters were used:

$N_x=181$ (number of nodes in x-direction)

$N_y=51$ (number of nodes in y-direction)

$\Delta x=0.1$ (step size in x-direction)

$\Delta y=0.1$ (step size in y-direction)

Conductor 1 is defined by nodes: $\begin{cases} i = 60..82 \\ j = 10 \end{cases}$

Conductor 2 is defined by nodes: $\begin{cases} i = 100..122 \\ j = 10 \end{cases}$

Dielectric region is defined by nodes: $\begin{cases} i = 1..179 \\ j = 1..10 \\ \epsilon_r = 4.7 \end{cases}$

where i represents node number in x-direction and j node number in y-direction.

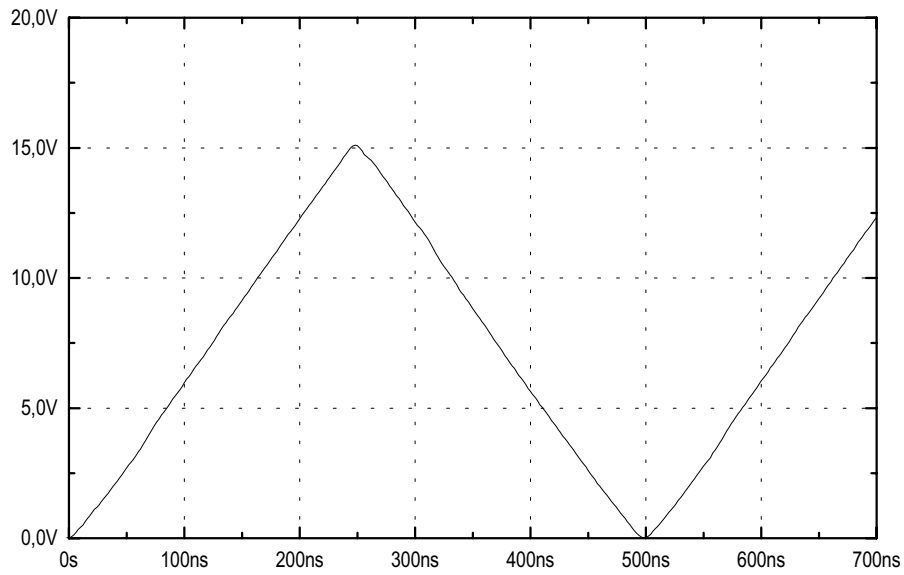


Figure 4:7. Excitation voltage waveform for the time domain experiment.

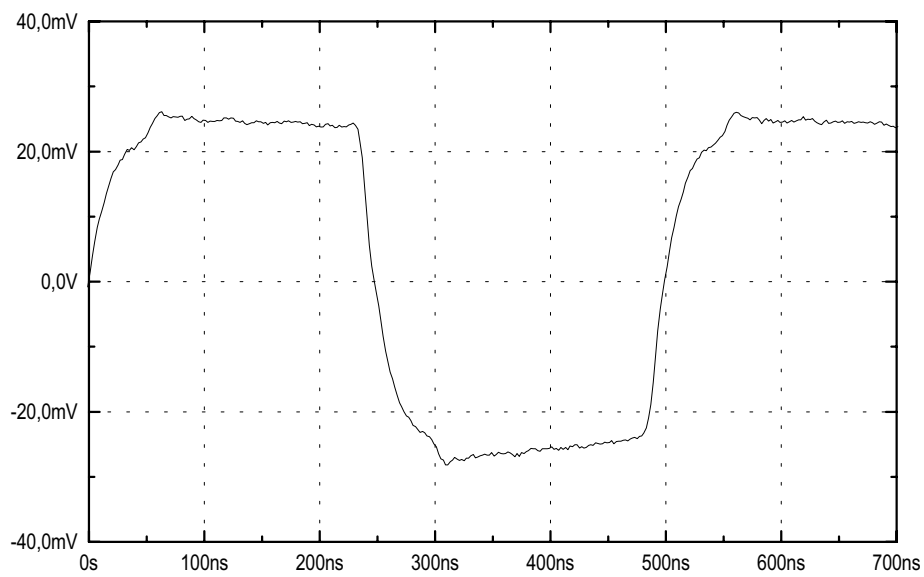


Figure 4:8. Measured far-end response for the time domain experiment.

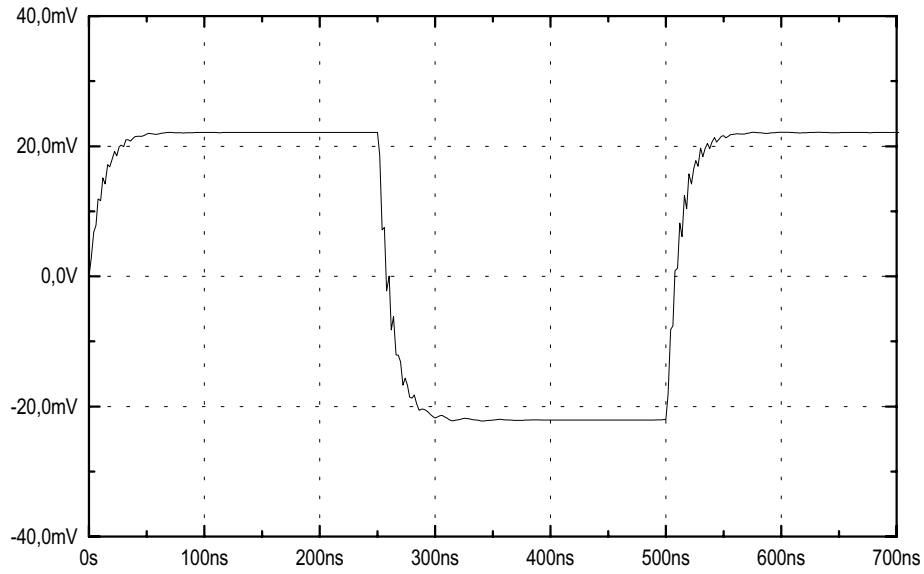


Figure 4:9. Computed far-end response for the time domain experiment.

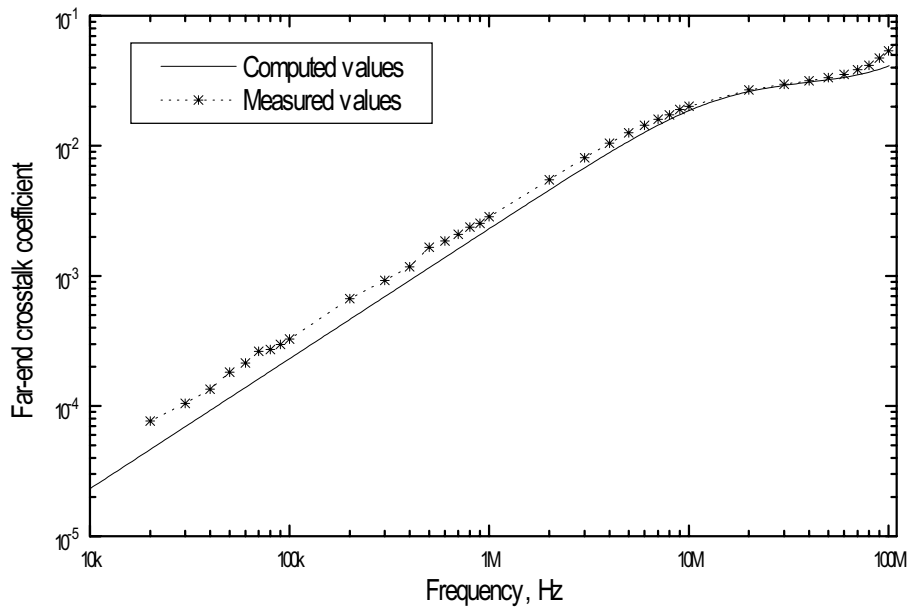


Figure 4:10. Computed and measured far-end crosstalk coefficient for the frequency domain experiment.

As another test case the same printed circuit board as shown in Fig. 4:6 was used but now terminated with 50 Ohm resistors instead of 1 kOhm. The program LC-Calc was used for determining the per unit length parameters as well as for generating the SPICE file. For this case the 2-line was described with seven lumped sections and the responses were measured with a network analyzer. The results are shown in Fig. 4:11 where an excellent agreement between measurements and computations can be observed for frequencies up to the first resonance. For higher frequencies the computed near-end response starts to deviate from measurements while the far-end response is still acceptable.

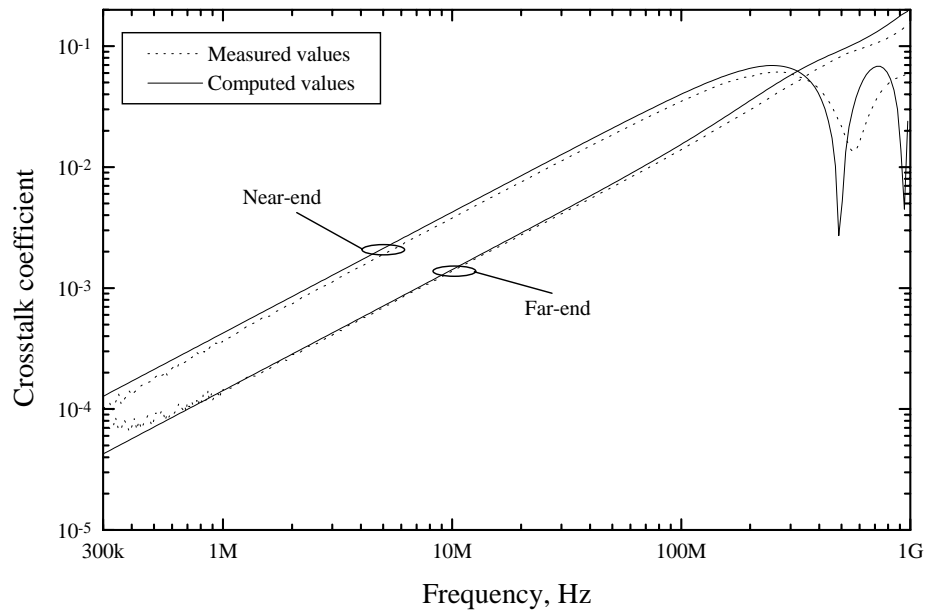


Figure 4:11. Computed and measured far-end crosstalk coefficient for the frequency domain experiment with 50 Ohm terminations.

5 Computed results

In this section a few computed results are presented in order to point out some important aspects of the crosstalk. All results presented in this section were obtained by first compute the per unit length parameters by the computer program LC-Calc and then let the program generate a lumped circuit file. Finally, the lumped circuit file was used as an input file for the circuit analyse program PSPICE.

5.1 General observations for a simple 2-line

As was seen in the previous section, about ten lumped circuit sections per wavelength should be used in order to predict the end-responses sufficiently accurate. This means that when we want to compute the responses in the time domain we should use as many sections as is required by the frequency content in the exciting voltage waveform. In order to give an idea of how we can determine the required frequency range for the model, a square wave is considered. The frequency spectrum for a square wave with a rise- and fall-time that are equal is shown in Fig. 5:1. As seen in Fig. 5:1 the amplitude falls of at a rate of 20 dB/decade for frequencies higher than $f_1 = 1/\pi T$ and as 40 dB/decade for frequencies higher than $f_2 = 1/\pi \tau_r$. The transfer function for the end-responses of a 2-line, both the near- and the far-end, are shown in Fig. 4:2-4:5. From these figures we can see that the end-responses increase as 20 dB/decade when the line is short compared with the wavelength and the envelopes to the responses are constant when the line is in the order of a wavelength and longer. We denote the break-frequency where the 20 dB/decade increase changes to constant with f_3 . The end-responses are given as the transfer function multiplied with the spectrum for the exciting voltage waveform. Thus, the following rule of thumb for how many sections that should be used in the lumped circuit model can be given:

- if $f_3 > f_2$ the model should be valid up to at least $5f_2$
- if $f_3 < f_1$ the model should be valid up to at least $5f_1$ or f_2 which ever is less

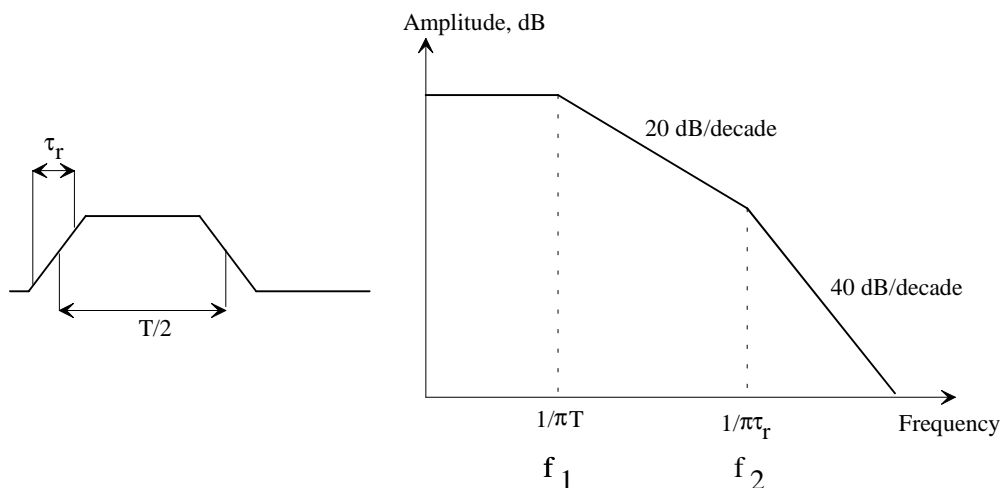


Figure 5:1. Frequency content for a square wave.

As an example of the time domain responses the same example as was treated in the previous section is considered. The configuration together with the two load cases that are treated are shown in Fig. 4:1. The excitation voltage waveform is a square wave with a

rise- and fall-time (0-100%) of 1 ns and the period 100 ns (simulating for instance a 10 MHz clock signal), the amplitude is 1 V. In the computation a five-section lumped circuit model was used and the results for the near- and far-end responses are shown in Fig. 5:2-5:5.

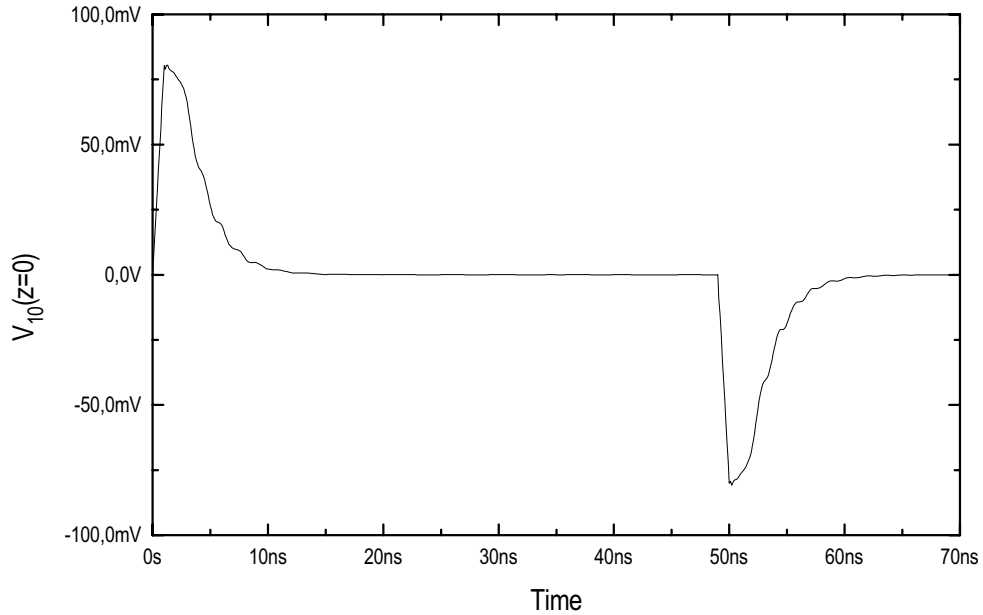


Figure 5:2. Near-end response for the configuration in Fig. 4:1 due to a 1 V, 10 MHz, 1 ns, square wave excitation, load case 1.

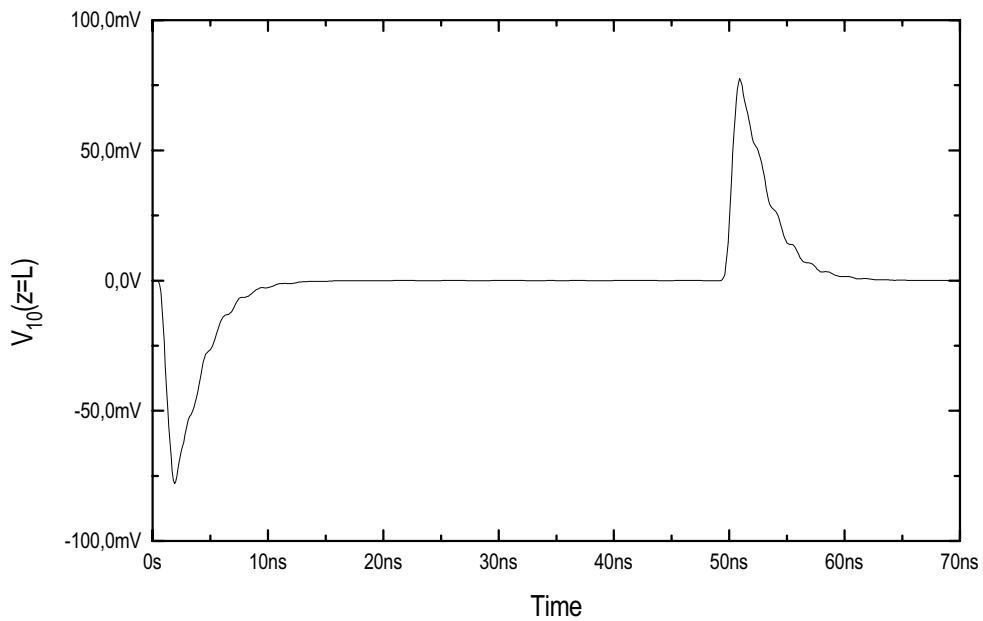


Figure 5:3. Far-end response for the configuration in Fig. 4:1 due to a 1 V, 10 MHz, 1 ns, square wave excitation, load case 1.

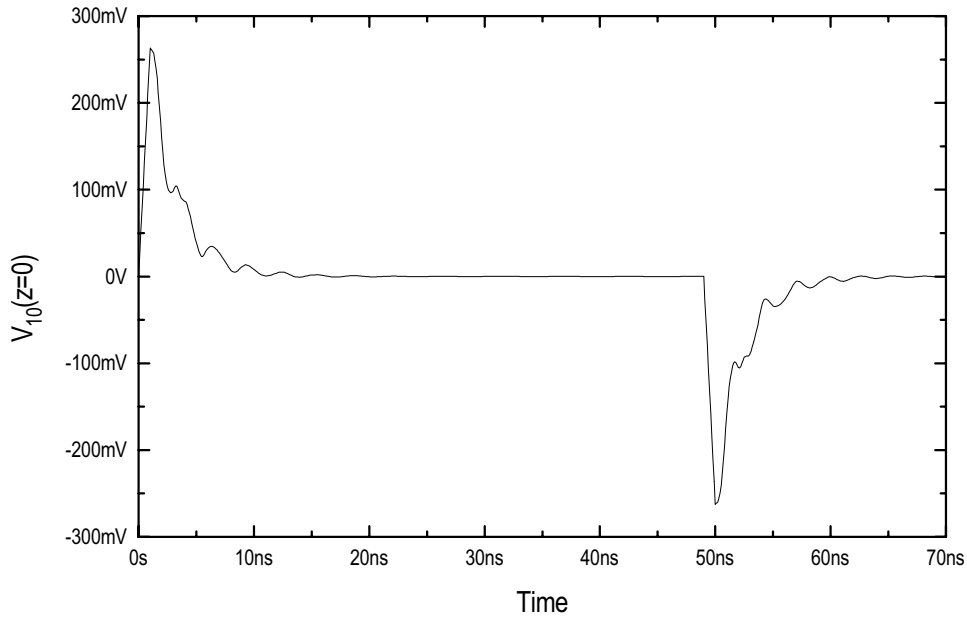


Figure 5.4. Near-end response for the configuration in Fig. 4:1 due to a 1 V, 10 MHz, 1 ns, square wave excitation, load case 2.

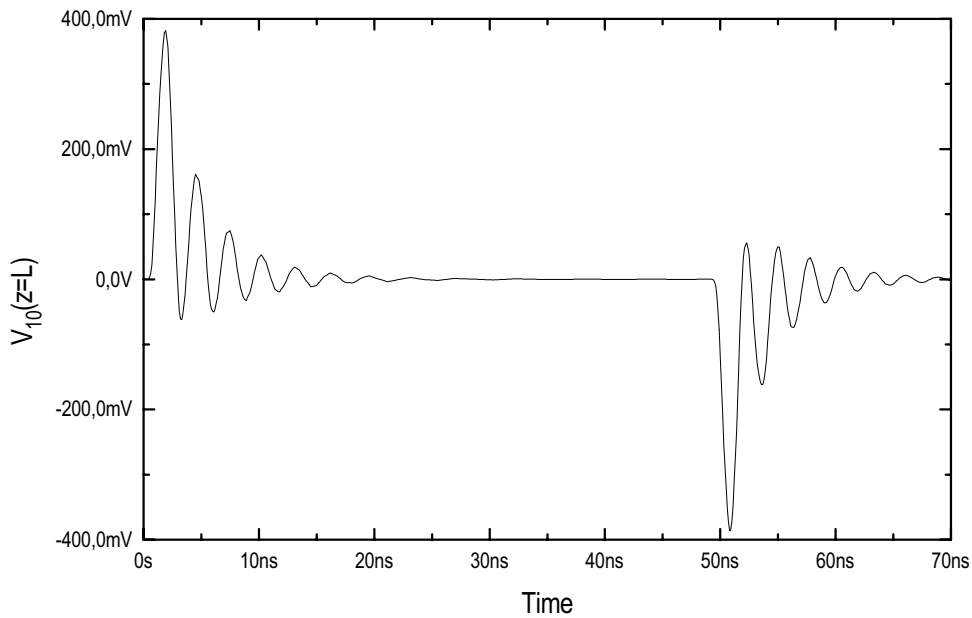


Figure 5.5. Far-end response for the configuration in Fig. 4:1 due to a 1 V, 10 MHz, 1 ns, square wave excitation, load case 2.

From the results in Fig. 5:2-5:5 we can see that the responses are due to the transition in the exciting voltage waveform (transition from low to high and vice versa). We can also see that the near-end response always have the same sign as the derivative of the exciting voltage waveform, i.e. positive going spike when the exciting waveform goes from low to high and negative when the exciting waveform goes from high to low. The far-end

response, on the other hand, has a sign which is dependent on the load conditions. When the load impedances are "low" the far-end response has the negative sign of the derivative of the exciting waveform and when the load impedances are "high" the same sign as the derivative. Since capacitive coupling is associated with voltages and inductive coupling is associated with currents, we can draw the conclusion that the far-end response has the same sign as the derivative of the exciting voltage waveform when the capacitive coupling dominates and the reverse sign when the inductive coupling dominates. This is an important observation which could be used if we want to know which type of coupling that dominates in a real case. By measuring the far-end response with an oscilloscope the dominating coupling type can easily be determined. The knowledge of which type of coupling that dominates can be essential if steps to reduce the coupling have to be taken.

When losses are introduced in the conductors, by a finite conductivity, the effect is that the crosstalk coefficients do not go to zero for decreasing frequency, as for the lossless case, but instead flattens out at a certain level. This level is due to the common impedance coupling and can easily be determined by a simple DC-computation. The effects of losses are shown in Fig. 5:6-5:7 where the configuration in Fig. 4:1 is considered again but now with a resistance of 200 m Ω /m in all three conductors.

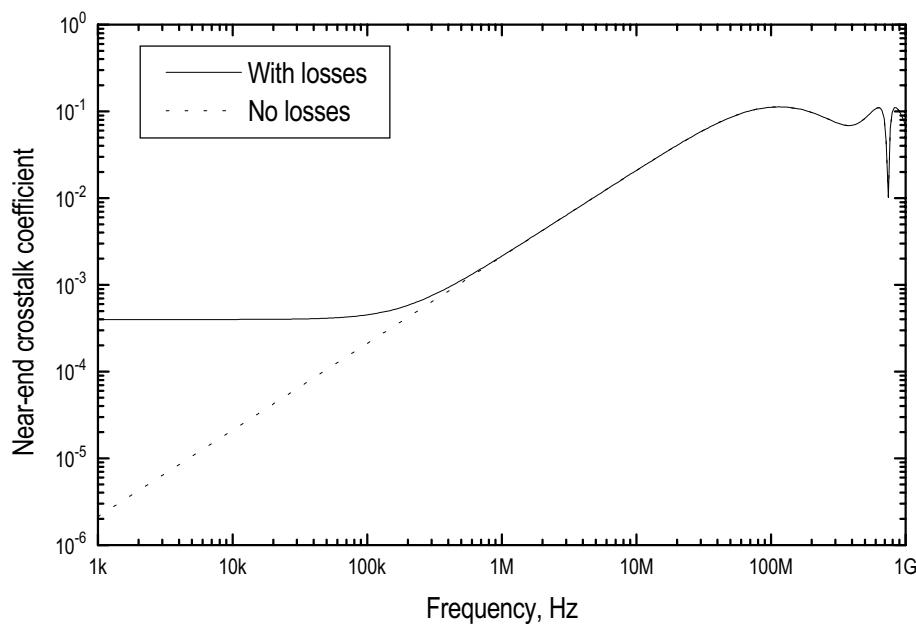


Figure 5:6. Near-end crosstalk coefficient, load case 1, $R_0=R_1=R_2=200$ m Ω /m, five lumped sections.

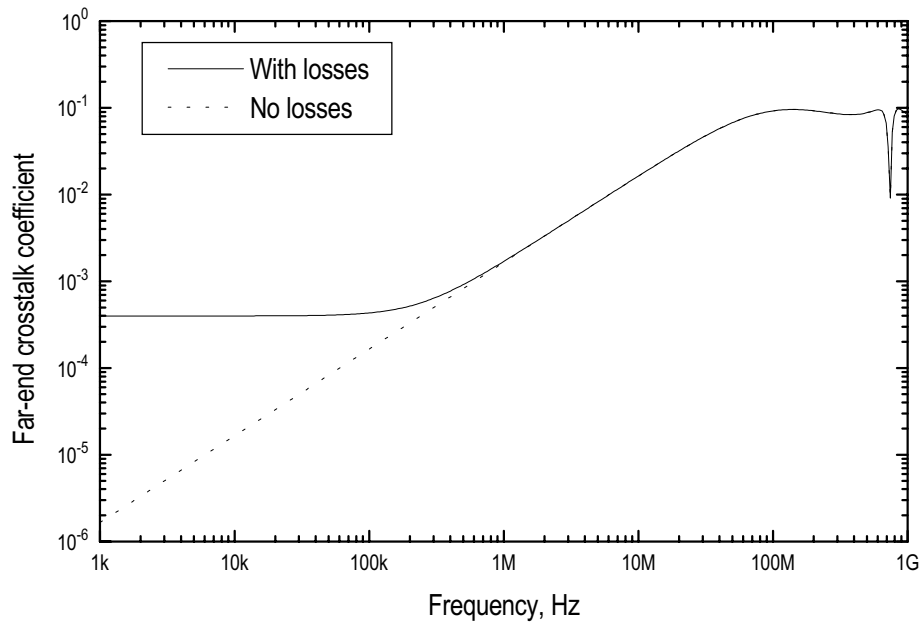


Figure 5:7. Far-end crosstalk coefficient, load case 1, $R_0=R_1=R_2=200\text{ m}\Omega/\text{m}$, five lumped sections.

5.2 Computed results for printed circuit boards

In this chapter a few different PCB-types and layouts are considered in order to show how the crosstalk on a PCB can be minimised.

5.2.1 Computed results for single layer PCBs

To start we consider the simple PCB shown in Fig. 5:8.

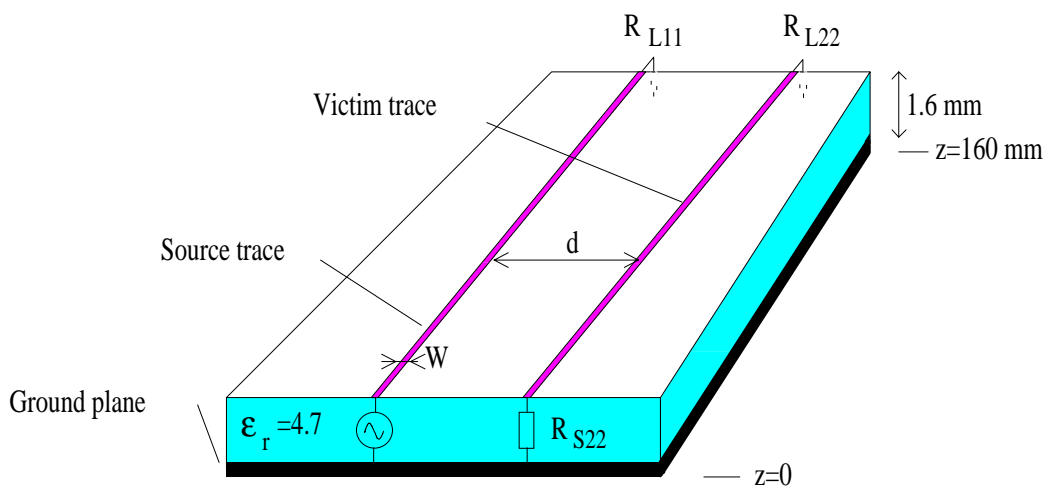


Figure 5:8. PCB with two traces.

To get a reference we first calculate the crosstalk coefficients for the configuration in Fig. 5:8, these are shown in Fig. 5:9-5:10.

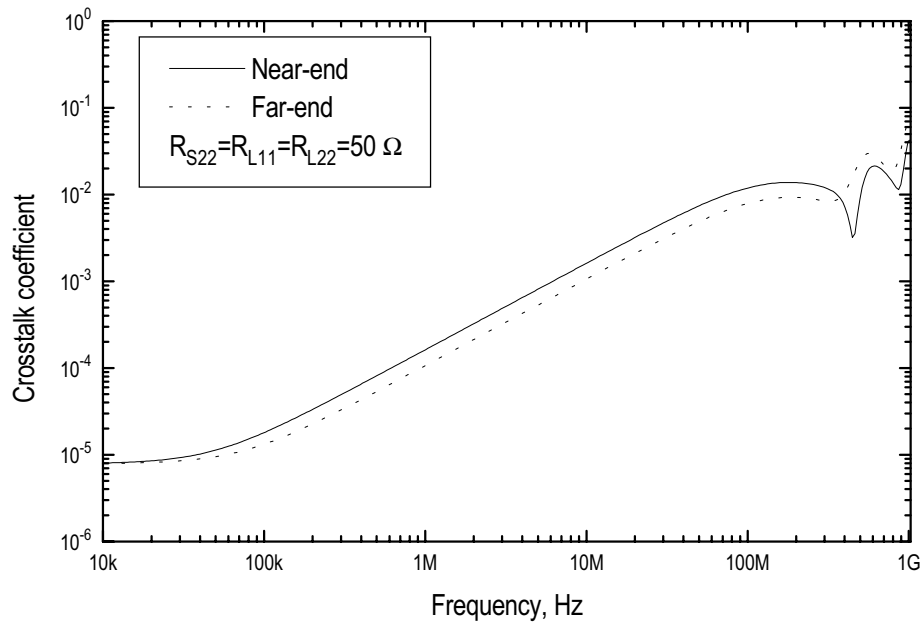


Figure 5:9. Near- and far-end crosstalk coefficients for load case 1 for the configuration shown in Fig. 5:8, $d=4$ mm, $W=1$ mm.

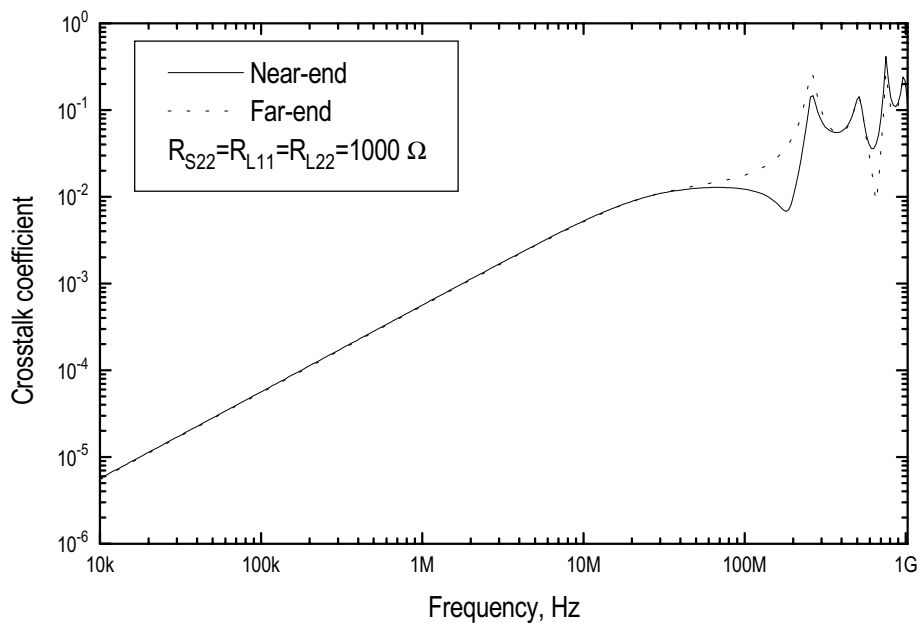


Figure 5:10. Near- and far-end crosstalk coefficients for load case 2 for the configuration shown in Fig. 5:8, $d=4$ mm, $W=1$ mm.

From time domain computations, which are not shown, it can be seen that inductive coupling dominates for load case 1 and capacitive coupling for load case 2 (see Ch. 5.1). In order to decrease the crosstalk we now introduce a shield-trace between the two traces, the resulting configuration is shown in Fig. 5:11.

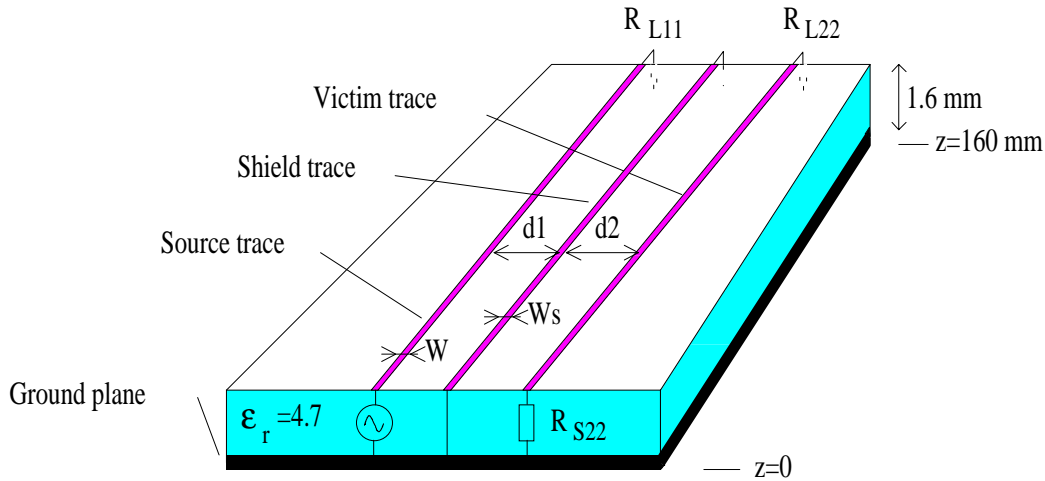


Figure 5:11. PCB with two traces and one shield-trace between.

When inductive coupling dominates the shield trace works because current flows in the shield trace and therefore the shield trace has to be grounded in both ends. On the other hand, when capacitive coupling dominates it is sufficient to ground the shield trace in only one end, i.e. if the traces are not too long in terms of the wavelength. For the results shown in Fig. 5:12-5:15 the shield trace is grounded in both ends.

The results shown in Fig. 5:12-5:15 are expressed as a relative crosstalk coefficient in decibel. The relative crosstalk coefficient is defined as the ratio between the crosstalk coefficient for the configuration in Fig. 5:11 to the crosstalk coefficient for the configuration in Fig. 5:8 ($CT_{Rel} = 20 \text{Log} \left(\frac{CT_{Fig.5.11}}{CT_{Fig.5.8}} \right)$). Thus, the results in Fig. 5:12-

5:15 represent the improvement by the introduction of the shield trace, for example a relative crosstalk coefficient of -20 dB means that the crosstalk is reduced by 20 dB by the use of the shield trace.

From the results below it can be seen that the shield trace can in fact increase the crosstalk, instead of decrease it, in some frequency ranges. This can be seen in Fig. 5:12 and 5:13 for load case 1, where inductive coupling dominates, for a frequency range approx. around 100 kHz. When capacitive coupling dominates, load case 2, the shield trace works as desired for all frequencies in the range 10 kHz - 1 GHz.

It can also be seen that it is advantageous to have a broad shielding trace and also to place it close to the generator trace instead of in the middle of the generator and victim traces.

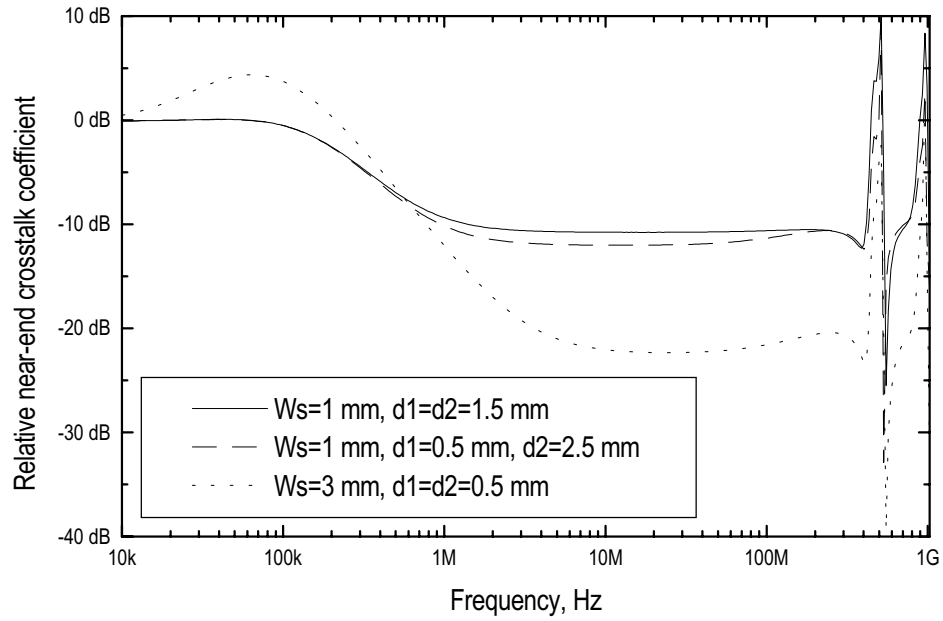


Figure 5:12. Relative near-end crosstalk coefficient, load case 1, $W=1$ mm.

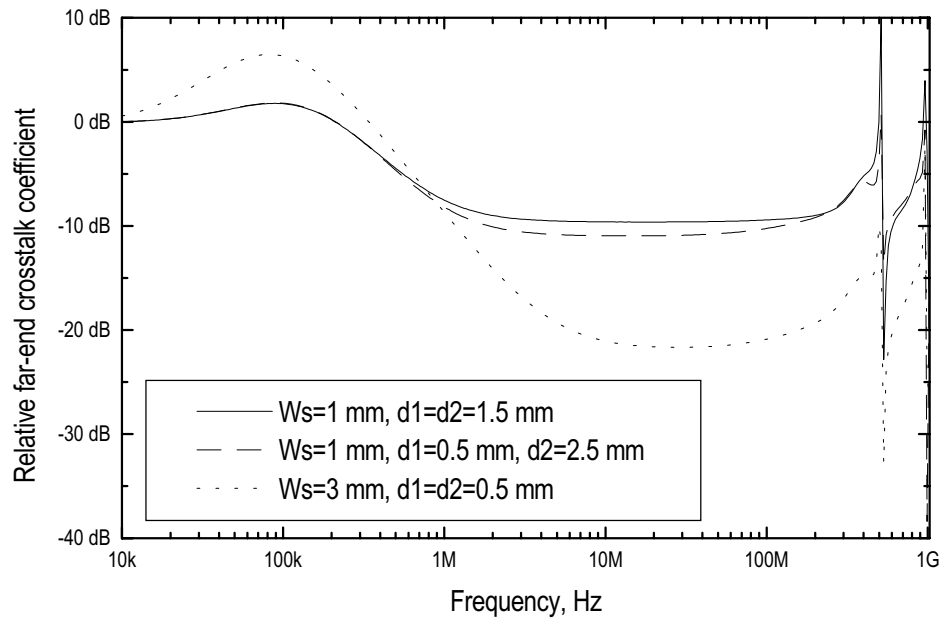


Figure 5:13. Relative far-end crosstalk coefficient, load case 1, $W=1$ mm.

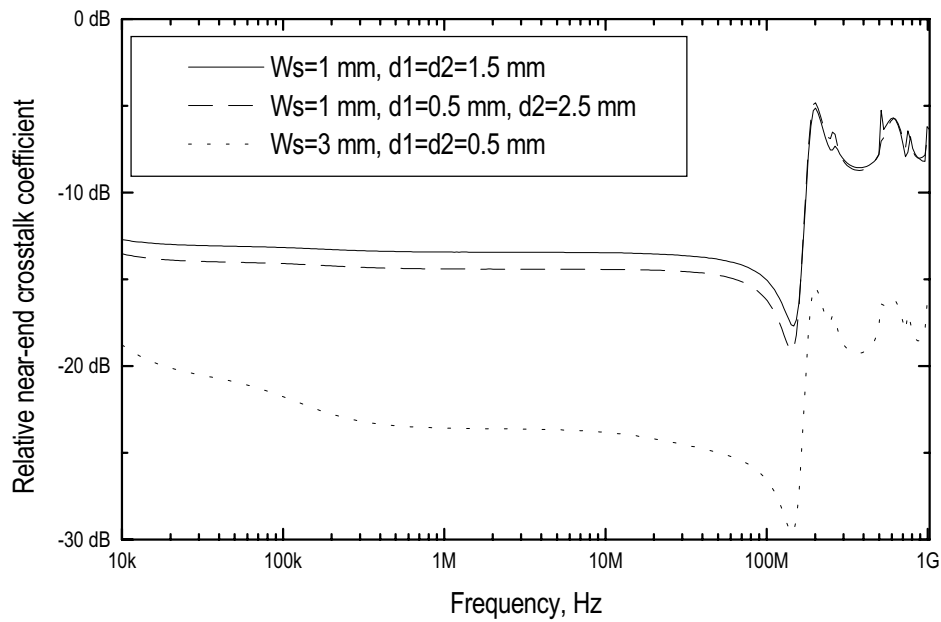


Figure 5:14. Relative near-end crosstalk coefficient, load case 2, $W=1$ mm.

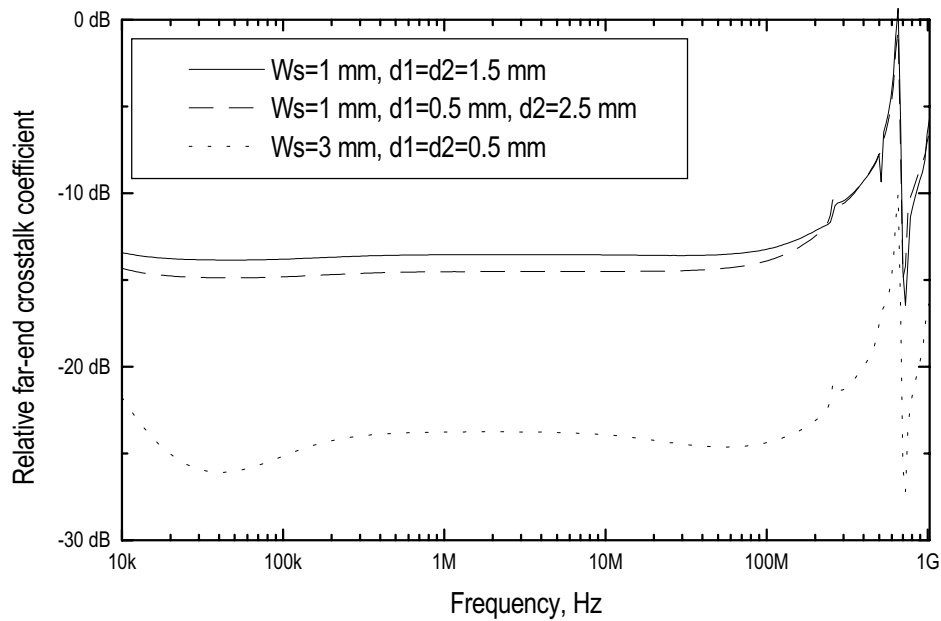


Figure 5:15. Relative far-end crosstalk coefficient, load case 2, $W=1$ mm.

To illustrate the effect of the shield trace in the time domain, a square wave with a rise- and fall-time (0-100%) of 1 ns, a period of 100 ns (10 MHz clock signal) and an amplitude of 1 V is used as the exciting voltage in Fig. 5:16.

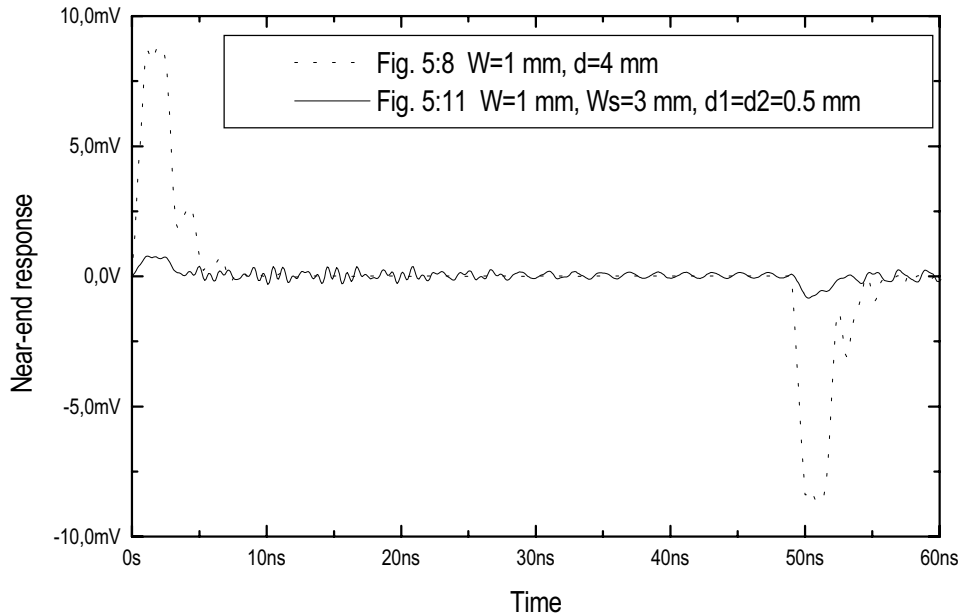


Figure 5:16. Time-domain near-end response for the configurations in Fig. 5:8 and 5:11 due to a 1 V, 10 MHz, 1 ns, square wave excitation, load case 1.

5.2.2 Computed results for multilayer PCBs

Multilayer PCBs are often used and therefore it can be interesting to analyse the crosstalk for this type of PCB. The cross section for a simple multilayer PCB, where the two outermost layers are ground planes, is shown in Fig. 5:17. This PCB can be thought as being made of two PCBs, as the one shown in Fig. 5:8, where one of the PCBs is turned upside down and placed on top of the other. It should be noted that the two outermost ground planes do not have to be grounded, so they can, for instance, be connected to DC-voltage sources. The configuration in Fig. 5:17 can also be thought as a part of a multilayer board with several other planes on top (or below) of the configuration in Fig. 5:17.

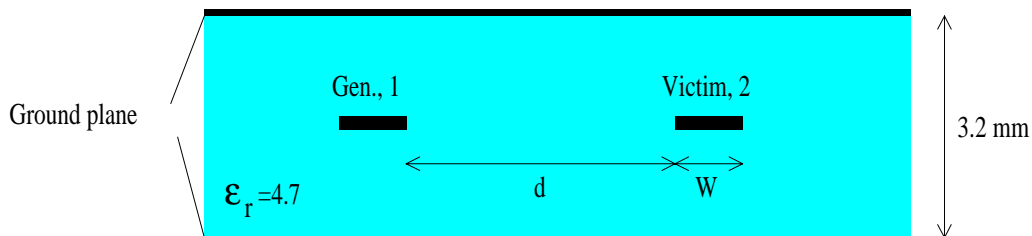


Figure 5:17. Cross section of a simple multilayer PCB (stripline).

The conductor marked *Gen* is connected to a voltage generator at one end and to a resistive load at the other end and the conductor marked *Victim* is connected to resistive loads at both ends. The lengths of the conductors are 0.16 m. The near- and far-end responses for the PCB in Fig. 5:17 are shown in Fig. 5:18-5:19. These responses should be compared with the curves in Fig. 5:9-5:10 for the PCB in Fig. 5:8. Due to the second ground plane on top of the traces, the crosstalk coefficients have decreased slightly for the multilayer board.

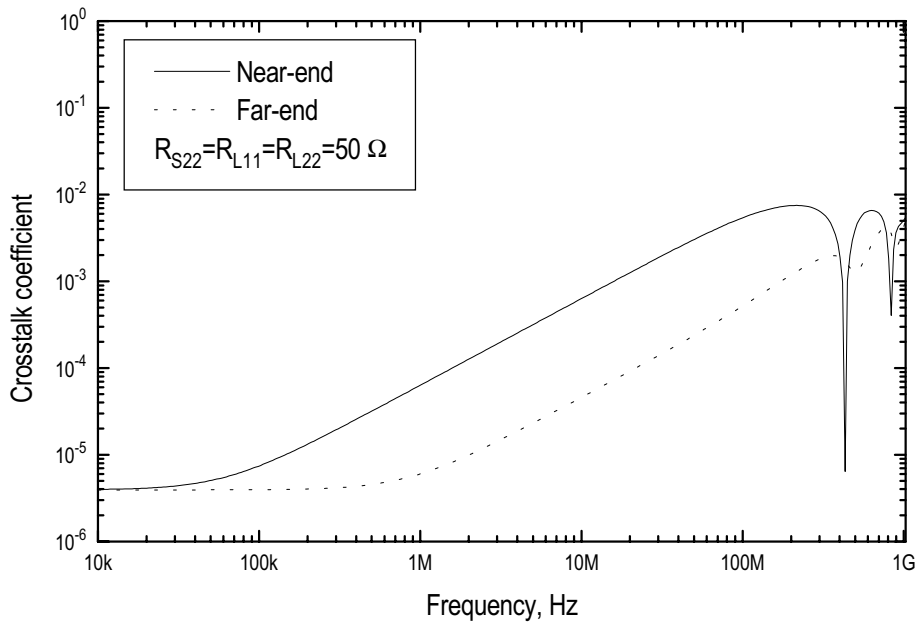


Figure 5:18. Near- and far-end crosstalk coefficients for load case 1 for the configuration shown in Fig. 5:17, $d=4$ mm, $W=1$ mm.

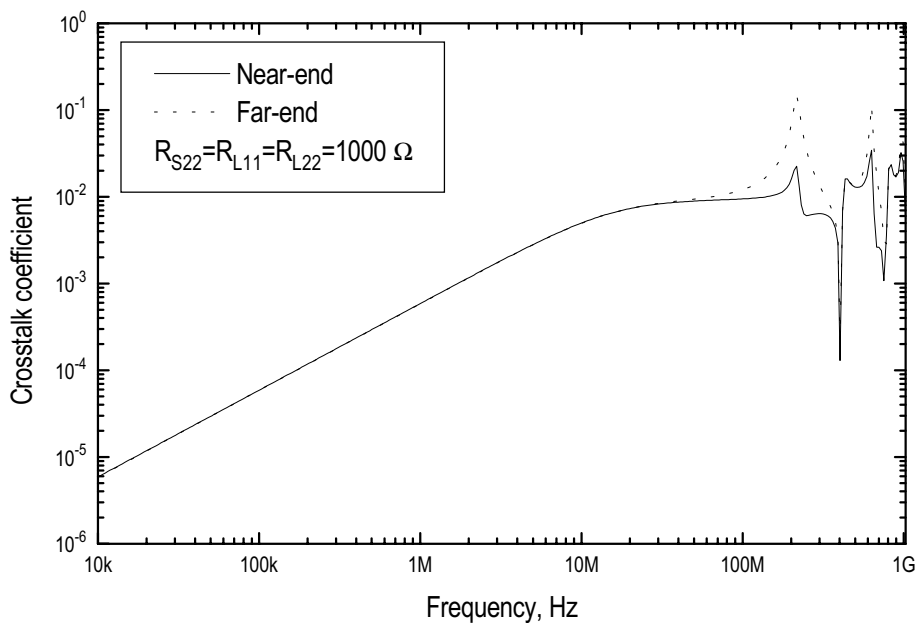


Figure 5:19. Near- and far-end crosstalk coefficients for load case 2 for the configuration shown in Fig. 5:17, $d=4$ mm, $W=1$ mm.

As for the single layer PCB a method to reduce the crosstalk is to introduce one or several shielding traces between the generator and the victim traces. Since we now are considering a multilayer board the shielding trace does not need to be on the same plane as the generator and victim traces, see Fig. 5:20. The effects of the different locations of the shielding trace are shown in Fig. 5:21-5:24.

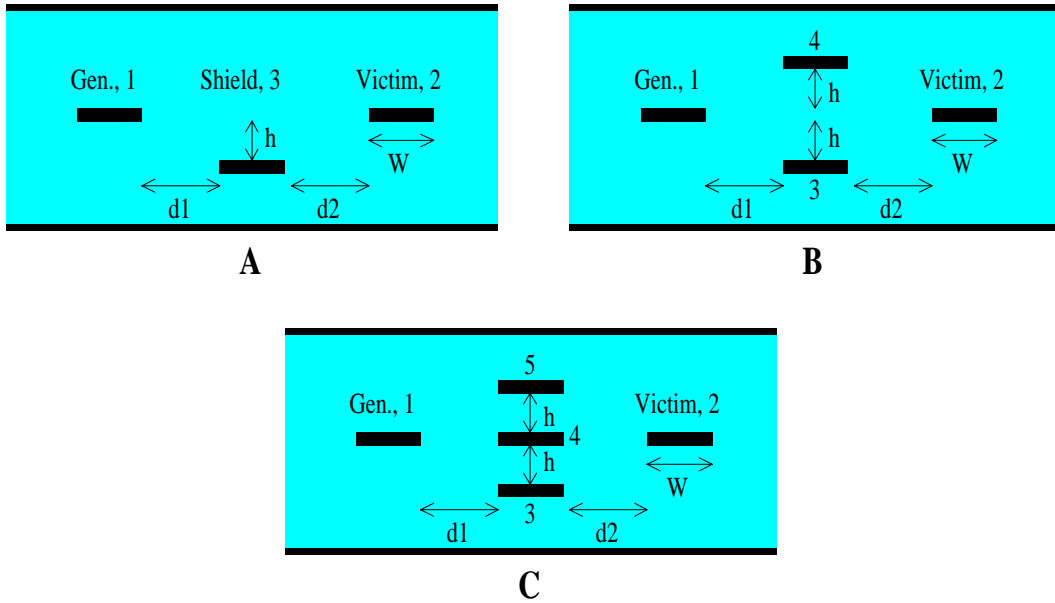


Figure 5:20. Placement of shielding traces for the multilayer board.

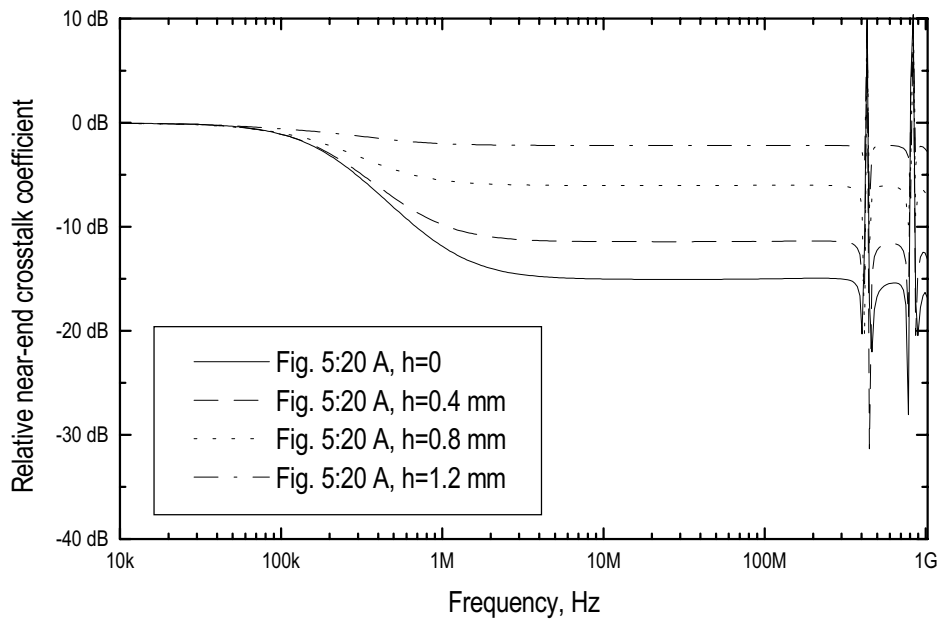


Figure 5:21. Relative near-end crosstalk coefficient for the configuration in Fig. 5:20 A, load case 1, $W=1$ mm, $d_1=d_2=1.5$ mm.

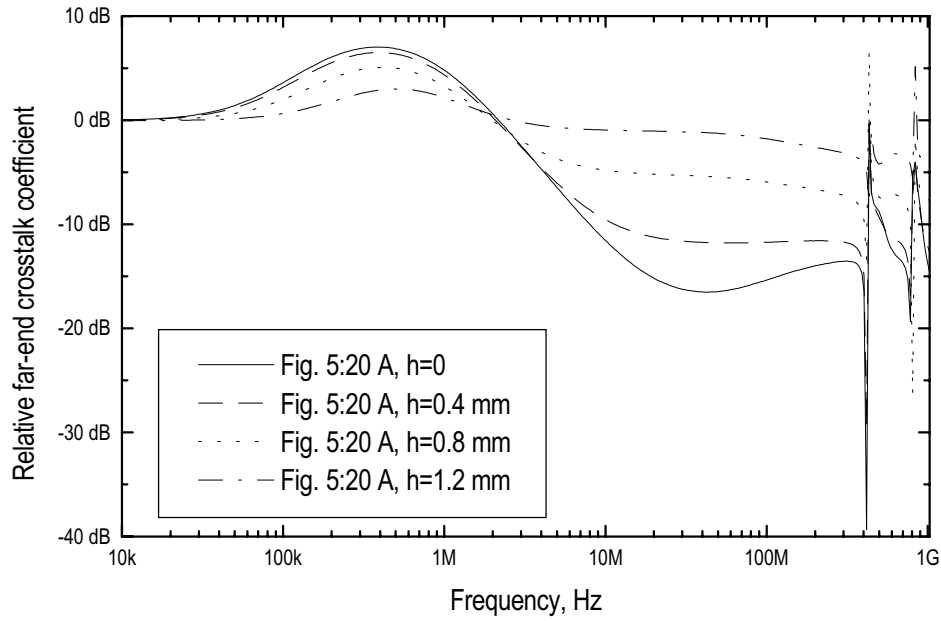


Figure 5:22. Relative far-end crosstalk coefficient for the configuration in Fig. 5:20 A, load case 1, $W=1$ mm, $d_1=d_2=1.5$ mm.

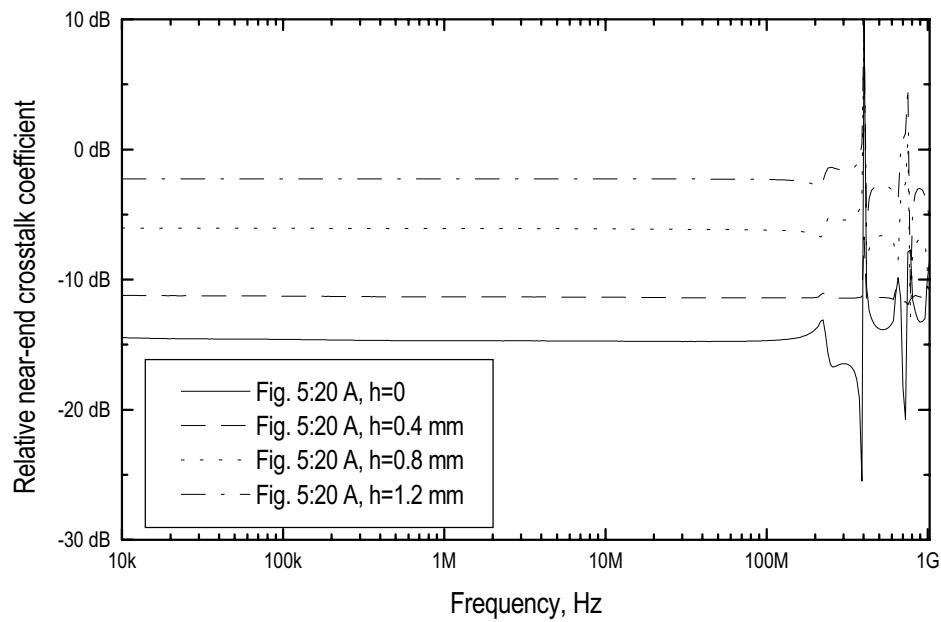


Figure 5:23. Relative near-end crosstalk coefficient for the configuration in Fig. 5:20 A, load case 2, $W=1$ mm, $d_1=d_2=1.5$ mm.

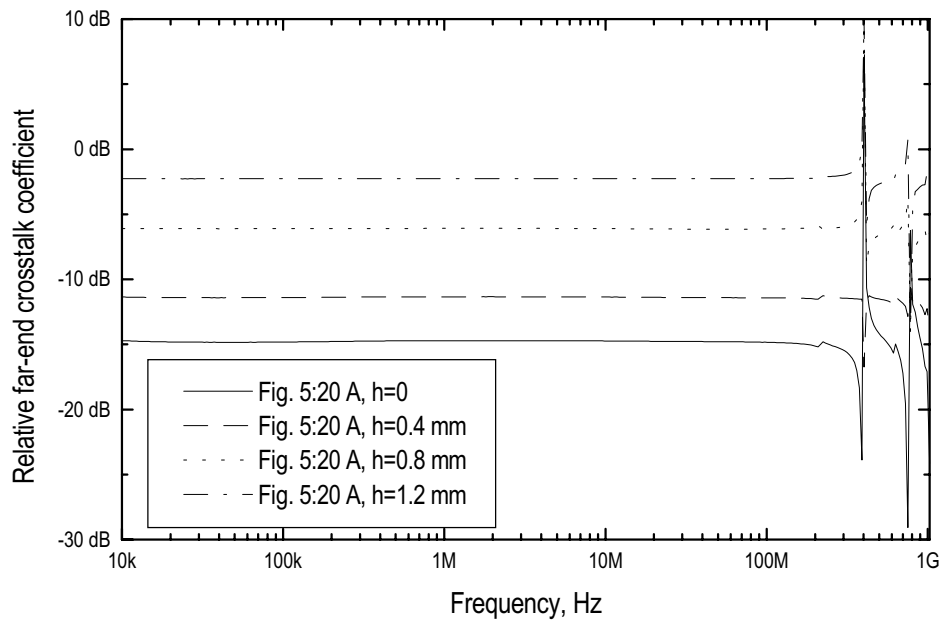


Figure 5:24. Relative far-end crosstalk coefficient for the configuration in Fig. 5:20 A, load case 2, $W=1$ mm, $d_1=d_2=1.5$ mm.

Again, we can see that the crosstalk can be increased, instead of decreased, when a shield trace is introduced. We can also see that the behaviour is "nicer" when capacitive coupling dominates, load case 2.

As expected, it is also seen that the best placement of the shielding trace is when it is placed in the same layer as the generator and victim traces.

The crosstalk can even be further decreased by the use of several shielding traces, examples are shown in Fig. 5:25-5:28. From the results it can be seen that the more shielding traces the lower crosstalk, especially when capacitive coupling dominates, load case 2.

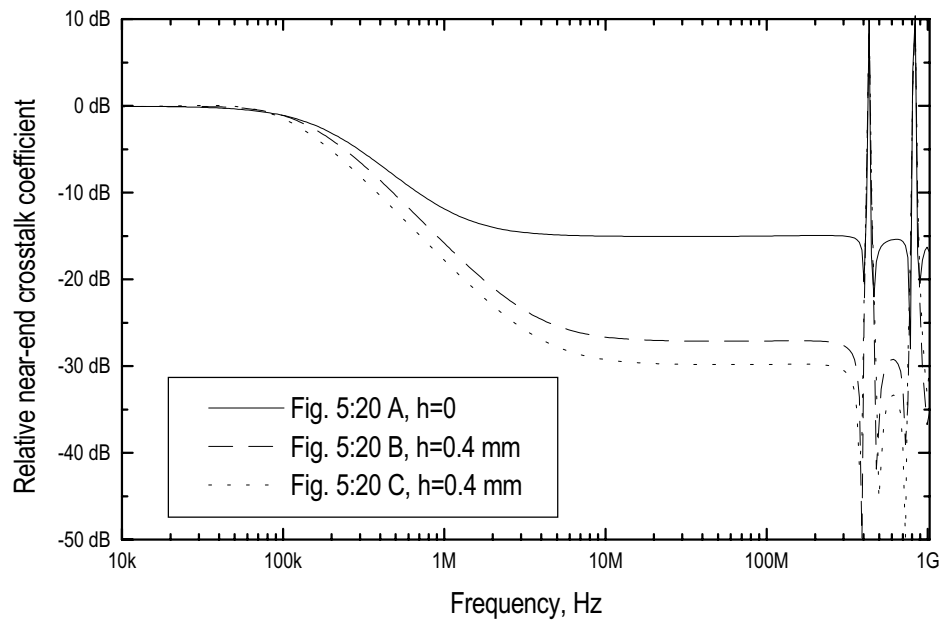


Figure 5:25. Relative near-end crosstalk coefficient for the configurations in Fig. 5:20 A, B and C, load case 1, $W=1$ mm, $d_1=d_2=1.5$ mm.

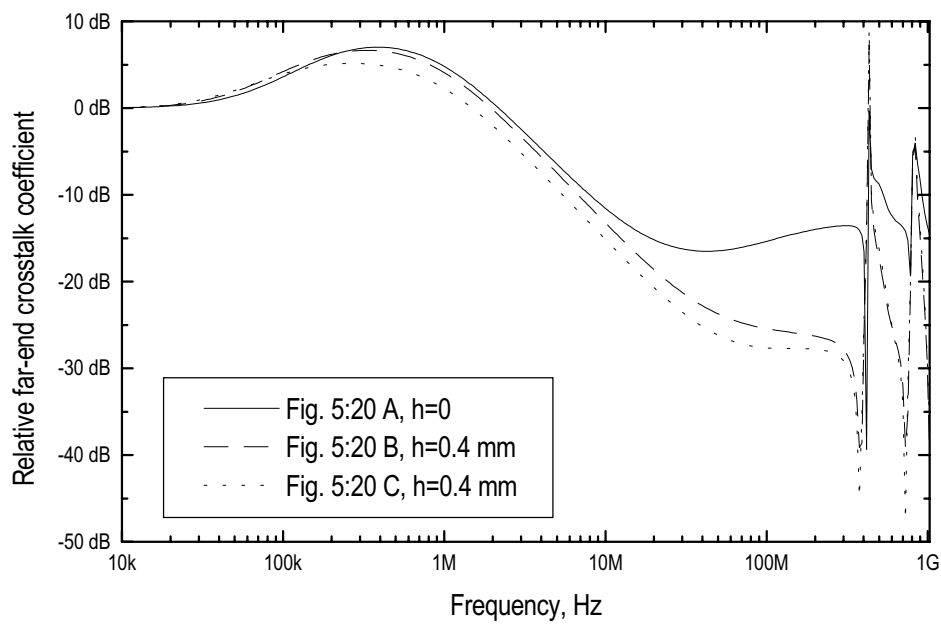


Figure 5:26. Relative far-end crosstalk coefficient for the configurations in Fig. 5:20 A, B and C, load case 1, $W=1$ mm, $d_1=d_2=1.5$ mm.

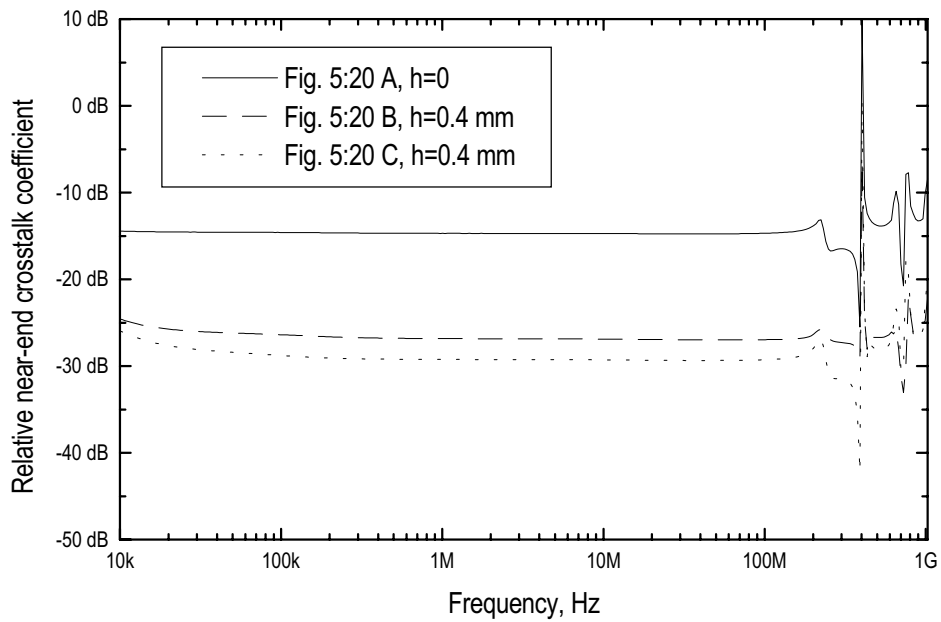


Figure 5:27. Relative near-end crosstalk coefficient for the configurations in Fig. 5:20 A, B and C, load case 2, $W=1$ mm, $d_1=d_2=1.5$ mm.

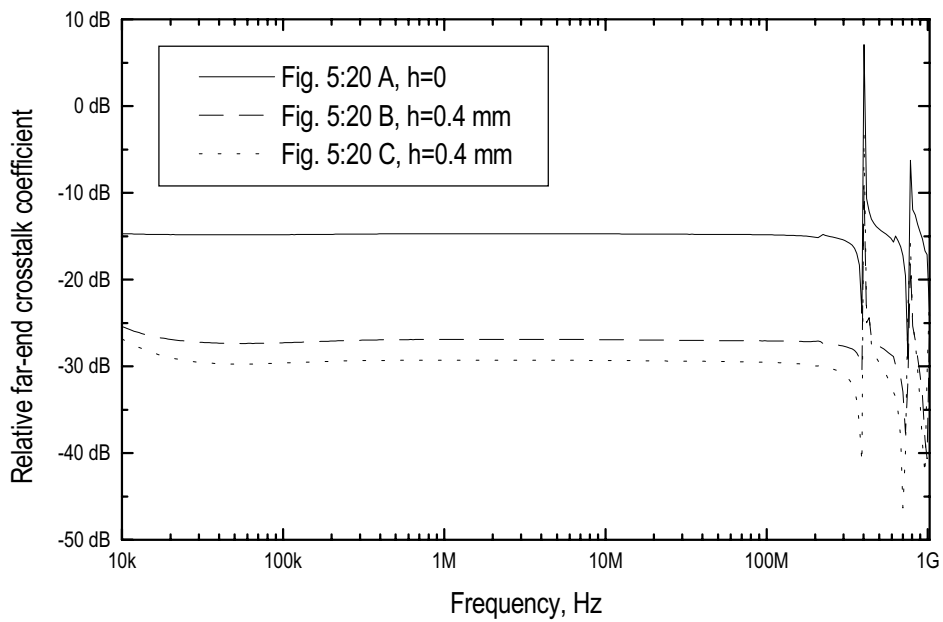


Figure 5:28. Relative far-end crosstalk coefficient for the configurations in Fig. 5:20 A, B and C, load case 2, $W=1$ mm, $d_1=d_2=1.5$ mm.

6 Conclusion

The presented method to use a lumped circuit equivalent for a multiconductor transmission line is a simple and efficient method to compute the crosstalk between adjacent traces on a PCB or conductors in a multiconductor cable. The main advantage with this method is that it is easy to compute the crosstalk, both in the time domain and in the frequency domain, for complicated structures with an ordinary circuit simulator. The results obtained by the method, when the per unit length parameters are calculated with a finite difference procedure, show a good agreement with measurements.

For a single layer PCB it was shown that a shielding trace between the generator and the victim trace could be used for decreasing the crosstalk. It was also seen that it is advantageous to place the shielding trace close to the generator trace instead of placing it in the middle of the generator and victim traces. For multilayer PCBs it was seen that the shielding trace does not even have to be in the same layer as the generator and the victim traces in order to reduce the crosstalk. For both cases it was seen that the shielding trace was most effective when the generator and victim traces were loaded with high impedances, i.e. when capacitive coupling dominates.

7 References

- [1] R. Laroussi and G.I. Costache, "Finite-Element Method Applied to EMC Problems", IEEE Transactions on Electromagnetic Compatibility, Vol. 35, No. 2, May 1993, pp. 178-184.
- [2] Wei et al., "Multiconductor Transmission Lines in Multilayered Dielectric Media", IEEE Transactions on Microwave Theory and Techniques, Vol. 32, No. 4, April 1984, pp. 439-450.
- [3] K.S.H. Lee, Editor, "EMP Interaction: Principles, Techniques and Reference Data", Air Force Weapons Laboratory Kirtland AFB, New Mexico, Dec. 1980.
- [4] C.R. Paul, "Introduction to Electromagnetic Compatibility", John Wiley & Sons, inc., 1992.
- [5] Pei-bai Zhou, "Numerical Analysis of Electromagnetic Fields", Springer-Verlag 1993.
- [6] R.F. Harrington, "Time-harmonic electromagnetic fields", McGraw-Hill, inc., 1961.

Appendix A Determination of the per unit length parameters

The per unit length parameters, the capacitances and the inductances, for a multiconductor transmission line can be determined by solving the two-dimensional electrostatic field problem for the geometry. When the electrostatic field problem is solved, i.e. the electric field pattern in the cross section of the transmission line is known, the capacitances can be calculated by the use of Gauss' law. If the medium in the cross section is free space the inductance matrix can easily be determined as, [2]: $[L] = \mu_0 \epsilon_0 [C_0]^{-1}$ where $[C_0]$ is the capacitance matrix. If the medium in the cross section is not free space we have to calculate the capacitance matrix taking the dielectric materials into account and also calculate the capacitance matrix for the case when all material is free space. The latter has to be calculated in order to calculate the inductance matrix.

In order to solve the electrostatic field problem for a two-dimensional region in the xy -plane that contains no free charges, we start with the following Maxwell equations:

$$\begin{cases} \mathbf{D} = \epsilon \mathbf{E} \\ \mathbf{E} = -\nabla V \\ \nabla \cdot \mathbf{D} = 0 \end{cases} \quad (\text{A1})$$

where ϵ is the permittivity and V is the electrostatic potential.

Insertion of the first and second relation into the last relation in (A1) gives for the homogeneous case:

$$\nabla \cdot (\epsilon \nabla V) = \nabla \cdot \left(\hat{x} \epsilon \frac{\partial V}{\partial x} + \hat{y} \epsilon \frac{\partial V}{\partial y} \right) = \epsilon \left[\frac{\partial^2 V}{\partial x^2} + \frac{\partial^2 V}{\partial y^2} \right] = 0 \quad (\text{A2})$$

In order to solve equation (A2) numerically on a computer we approximate the derivatives by finite differences. Thus, the following approximations are introduced:

$$\begin{aligned} \frac{\partial V}{\partial x} &\approx \frac{V_{i+1,j} - V_{i-1,j}}{2\Delta x}, & \frac{\partial V}{\partial y} &\approx \frac{V_{i,j+1} - V_{i,j-1}}{2\Delta y} \\ \frac{\partial^2 V}{\partial x^2} &\approx \frac{V_{i+1,j} + V_{i-1,j} - 2V_{i,j}}{\Delta x^2}, & \frac{\partial^2 V}{\partial y^2} &\approx \frac{V_{i,j+1} + V_{i,j-1} - 2V_{i,j}}{\Delta y^2} \end{aligned} \quad (\text{A3})$$

where the indexes i and j are defined as shown in Fig. A1. The equations (A2) and (A3) stipulate that the potential at the node i,j can be determined by the knowledge of the potentials at the four surrounding nodes. Thus, by defining a number of nodes in the region that we are interested in and by stepping through the nodes we can determine the potential at all nodes. In order to do this we need to have a finite region with a closed boundary and we also have to define the potentials on the boundary, i.e. we put them to zero. If we have an infinite region (e.g. a microstrip) we have to truncate the region and let the potential be zero on the enclosing boundary. This will in practice be no problem since we can make the truncated region sufficiently large so that it will not influence the results.

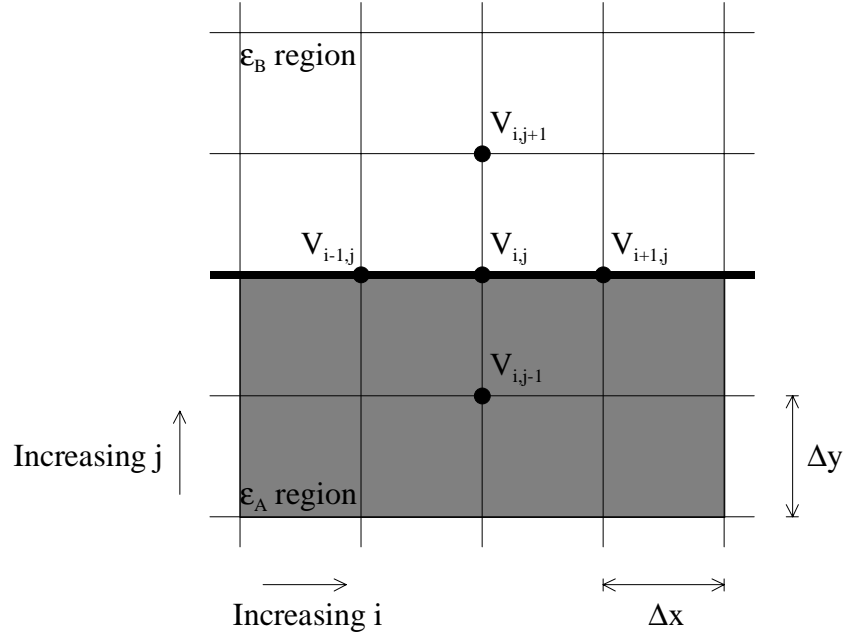


Figure A1. A part of the finite difference mesh.

Insertion of the approximations (A3) in equation (A2) gives the following expression, which is suitable for computer implementation:

$$V_{i,j} = C_y V_{i-1,j} + C_y V_{i+1,j} + C_x V_{i,j-1} + C_x V_{i,j+1} \quad (\text{A4})$$

where

$$C_x = \frac{\Delta x^2}{2(\Delta x^2 + \Delta y^2)}, \quad C_y = \frac{\Delta y^2}{2(\Delta x^2 + \Delta y^2)}$$

The finite difference equation (A4) can easily be implemented on a computer and solved by an iterative process. Perhaps, the most straight forward way to implement (A4) is to define two arrays, one for the potentials at iteration n and one for the potentials at the iteration $n+1$. The right hand side of (A4) is then associated with iteration n and the left hand side of (A4) with iteration $n+1$. Now, by stepping through the whole mesh and when this is finished swapping the arrays, one complete iteration is performed. Continuing this process until the values do not change any more gives the potentials at every node in the mesh. This procedure is called the Jacobian iterative method. One of the disadvantages with this method is that two arrays containing the potentials at every node have to be stored.

Another, more efficient, method is to use the potentials previously computed as soon as they are available. Depending on how the potentials are updated, i.e. how the stepping through the mesh is performed, the finite difference equation (A4) can be written in different ways, for example as in (A5).

$$V_{i,j}^{n+1} = C_y V_{i-1,j}^{n+1} + C_y V_{i+1,j}^n + C_x V_{i,j-1}^{n+1} + C_x V_{i,j+1}^n \quad (\text{A5})$$

where the superscript n stands for iteration n . In (A5) we have assumed that the updating of the node potentials is done from the left to the right starting with the bottom row, i.e.

increasing i before j . The advantage of this method, which is called the Gauss-Seidel iteration procedure, is that now we only have to store one array for the node potentials.

When we have one or several sub-regions with different permittivities within the problem space special care must be taken. The constraint we must put on the solution is that the normal component of the electric flux density, \mathbf{D} , must be continuous across the boundary. For the case of a horizontal boundary between two sub-regions with dielectric constants ϵ_A and ϵ_B , Fig. A1, equation (A5) has to be modified. Referring to Fig. A1 the electrostatic potential in the region above the interface between the two dielectric materials satisfies Laplace equation $\nabla^2 V^B = 0$. And similarly for the electrostatic potential in the region below the interface $\nabla^2 V^A = 0$, where superscripts A and B denote respective dielectric region. Treating both regions as they both are homogenous and filled with material with dielectric constants ϵ_A and ϵ_B , respectively, equation (A5) can be written as (with the iteration number omitted):

$$V_{i,j}^{A,B} = C_y V_{i-1,j}^{A,B} + C_y V_{i+1,j}^{A,B} + C_x V_{i,j-1}^{A,B} + C_x V_{i,j+1}^{A,B} \quad (\text{A6})$$

In equation (A6) $V_{i,j-1}^B$ and $V_{i,j+1}^A$ are fictitious and can be eliminated by the following relations:

$$\begin{cases} V_{i,j}^A = V_{i,j}^B = V_{i,j} \\ V_{i-1,j}^A = V_{i-1,j}^B = V_{i-1,j} \\ V_{i+1,j}^A = V_{i+1,j}^B = V_{i+1,j} \\ \epsilon_A (V_{i,j+1}^A - V_{i,j-1}^A) = \epsilon_B (V_{i,j+1}^B - V_{i,j-1}^B) \end{cases}$$

where the last relation represent the requirement of continuous normal component of the electric flux density across the boundary. Finally, by multiplying equation (A6) with $(\epsilon_A + \epsilon_B)$ and using the above boundary conditions we obtain

$$V_{i,j}^{n+1} = C_y V_{i-1,j}^{n+1} + C_y V_{i+1,j}^n + C_x \frac{2\epsilon_A}{\epsilon_A + \epsilon_B} V_{i,j-1}^{n+1} + C_x \frac{2\epsilon_B}{\epsilon_A + \epsilon_B} V_{i,j+1}^n \quad (\text{A7})$$

It should be noted that equation (A7) is valid also for homogenous regions, i.e. when $\epsilon_A = \epsilon_B$. Vertical boundaries can be treated in an analogous way.

The convergence speed of both the Jacobian and the Gauss-Seidel iteration procedures is quite slow. However, the convergence speed can be increased by using a so-called over-relaxation method, [5]. For this method we define the residual for the potential as the difference between the values for two successive iterations. Thus, $R_{i,j} = V_{i,j}^{n+1} - V_{i,j}^n$. Now, by introducing a relaxation factor α and letting the new potential value be equal to the old value plus the residual times the relaxation factor, the convergence speed can be increased. Thus, $V_{i,j}^{n+1} = V_{i,j}^n + \alpha R_{i,j}$ where the relaxation factor should be greater than or equal to unity and be smaller than two. If $\alpha = 1$ the equation reduces to (A7) and if $\alpha = 2$ the iteration becomes divergent. This over-relaxation method is known as "the successful over relaxation" method (SOR).

Of course, it can be difficult to find the optimal value for the relaxation factor and therefore the following formula can be helpful for the initial guess, [5]:

$$\alpha_0 = 2 - \pi \sqrt{2 \left(\frac{1}{N_x^2} + \frac{1}{N_y^2} \right)} \quad (\text{A8})$$

where a rectangular finite difference mesh is assumed and $(N_x + 1)$, $(N_y + 1)$ are the number of nodes in the x- and y-directions respectively.

To illustrate the gain in convergence speed by using the SOR the problem in Fig. A2 is considered.

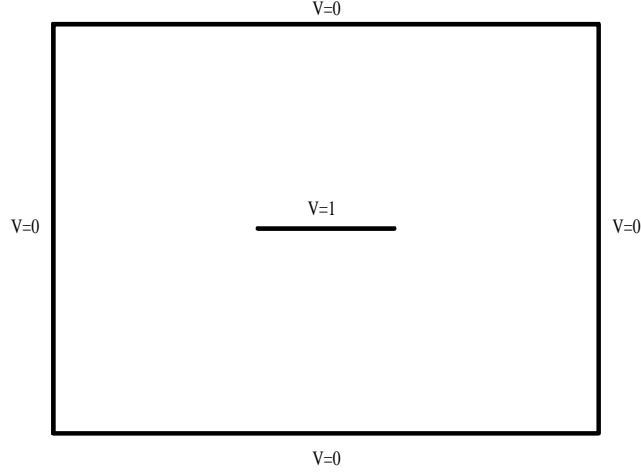


Figure A2. Example problem for illustrating the efficiency of SOR.

The rectangular region in Fig. A2 is divided into 40 nodes in the x-direction and 30 in the y-direction, the potential on the outer boundary is forced to zero and the potential on the strip in the region is set to unity. The strip is defined as $i = 15..25$, $j = 15$ and the convergence criteria is 10^{-6} , i.e. the maximum allowed difference between potentials for two successive iterations at all nodes. The convergence rate for different values of the relaxation factor is shown in table A1.

Relaxation factor, α	No. of iterations	Relaxation factor, α	No. of iterations
1.00	495	1.77	62
1.50	178	1.78	64
1.70	93	1.809	73
1.76	63	1.98	615

Table A1. Convergence rate for the problem in figure A2.

As seen in table A1 the optimal value for the relaxation factor is close to 1.77. The value 1.809 is the value predicted by the formula (A8).

Now, when the potential distribution in the region can be computed with the method discussed above, the question is how to use the method in order to calculate the capacitance and inductance matrices. The elements in the capacitance matrix are defined by, [1]: $C_{ij} = \frac{Q_i}{V_j} \Big|_{V_m=0, m \neq j}$ where Q_i is the total charge on conductor i due to the voltage on conductor j . The element in the capacitance matrix satisfies the following relations:

$$\begin{cases} C_{ii} \geq 0 \\ C_{ij} \leq 0 \text{ for } i \neq j \\ C_{ij} = C_{ji} \end{cases}$$

The total charge enclosed by a closed surface can be computed by Gauss' law, [6]. For the two-dimensional case, as treated here, the charge is the charge per unit length and the surface integral is reduced to a line integral. Thus, $Q_i = -\oint_{l_i} \epsilon \nabla V \cdot \hat{n} dl_i$ where l_i is a closed line around conductor i , \hat{n} is an outward directed unit vector and V is the potential distribution.

Thus, in order to calculate all elements in the capacitance matrix for a configuration with N conductors, we have to compute the potential distribution $V(x, y)$ N times (with different boundary conditions) and perform the integration according to Gauss' law $N + (N - 1) + \dots + 1$ times. As an example, the procedure for the configuration in Fig. A3 will be as follows:

1. Compute the potential distribution when the potential on conductor 1 is unity and zero on conductor 2.
2. Compute the charges on conductor 1 and 2.
3. Compute the capacitances $C_{11}, C_{12} = C_{21}$
4. Compute the potential distribution when the potential on conductor 1 is zero and unity on conductor 2.
5. Compute the charge on conductor 2.
6. Compute the capacitance C_{22}

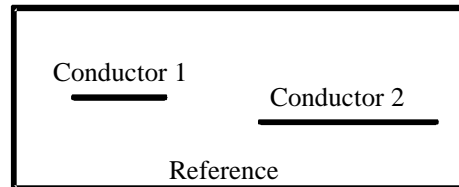


Figure A3. A configuration with two conductors (a 2-line).

The inductance matrix can be computed as, [2]: $[L] = \mu_0 \epsilon_0 [C_0]^{-1}$ where $[C_0]$ is the capacitance matrix when all dielectric material in the cross section is replaced by free space.

Appendix B The computer code LC-Calc

A computer program called LC-Calc based on the theory discussed in appendix A has been developed. The computer program can be used on an ordinary PC and runs under Windows 95 or NT 4.0 or later.

The program first calculates the potential distribution when one of the conductors is set to a unit potential and all others to zero potential. When this is done the program computes the charges on all conductors by integrating around them. This procedure is repeated until all conductors have had the unit potential. The capacitance matrix is saved in a file and if the free space capacitance matrix is computed the program also computes the inductance matrix by matrix inversion. The program can also generate a SPICE circuit file containing π -sections based upon the computed per unit-length parameters.

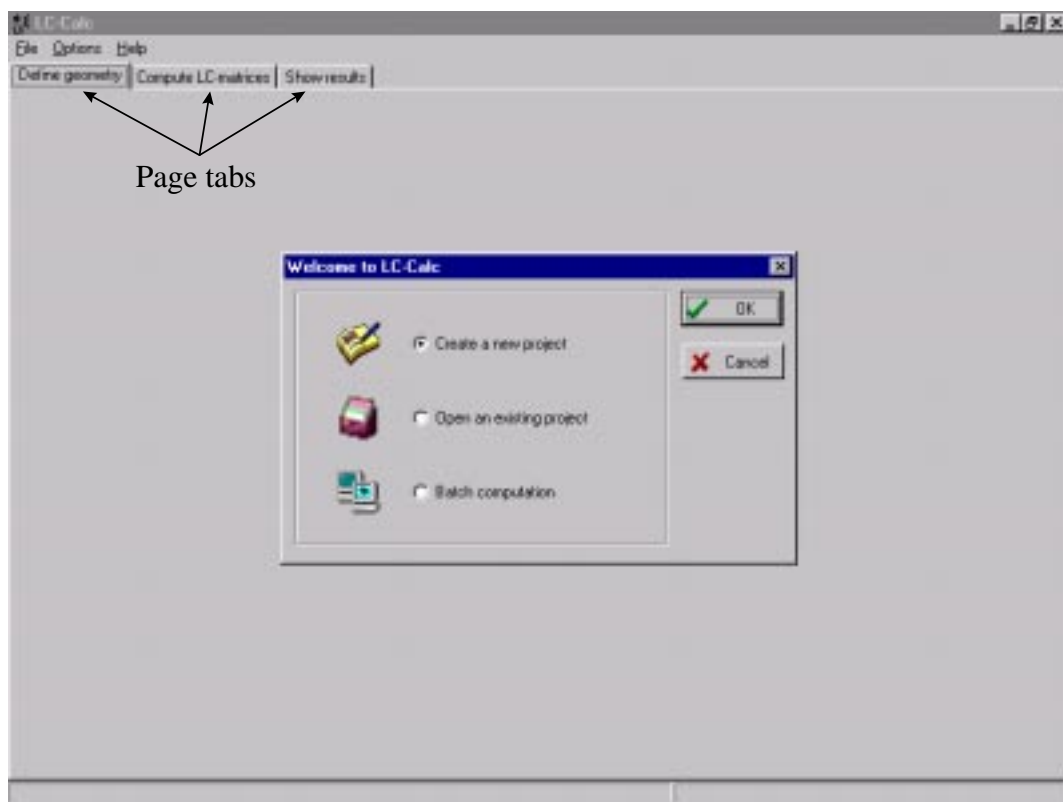


Figure B1. The screen as it appears when LC-Calc is started.

As soon as the program is started the screen will appear as a tabbed notebook with three pages; Define geometry, Compute LC-matrices and Show results, Fig. B1. Switching between these pages is done by clicking on the corresponding page tab. Clicking a page tab will also have the effect of restoring the screen after that e.g. a dialog box has destroyed the contents on the screen.

Define geometry page

On this page the cross section of the homogeneous transmission line to be analysed is defined. The boundary to the rectangular computation domain is shown as a solid black line. The potential is set to zero on this boundary so it can be thought of as a metallic conducting box enclosing the transmission line. If a problem with an open boundary is to be analysed, such as e.g. an unshielded microstrip line, the distance between the boundary

and the lines of the transmission line has to be sufficiently large in order not to affect the results. Since the L- and C-matrices mainly are determined by near-field effects this is no problem in practice.

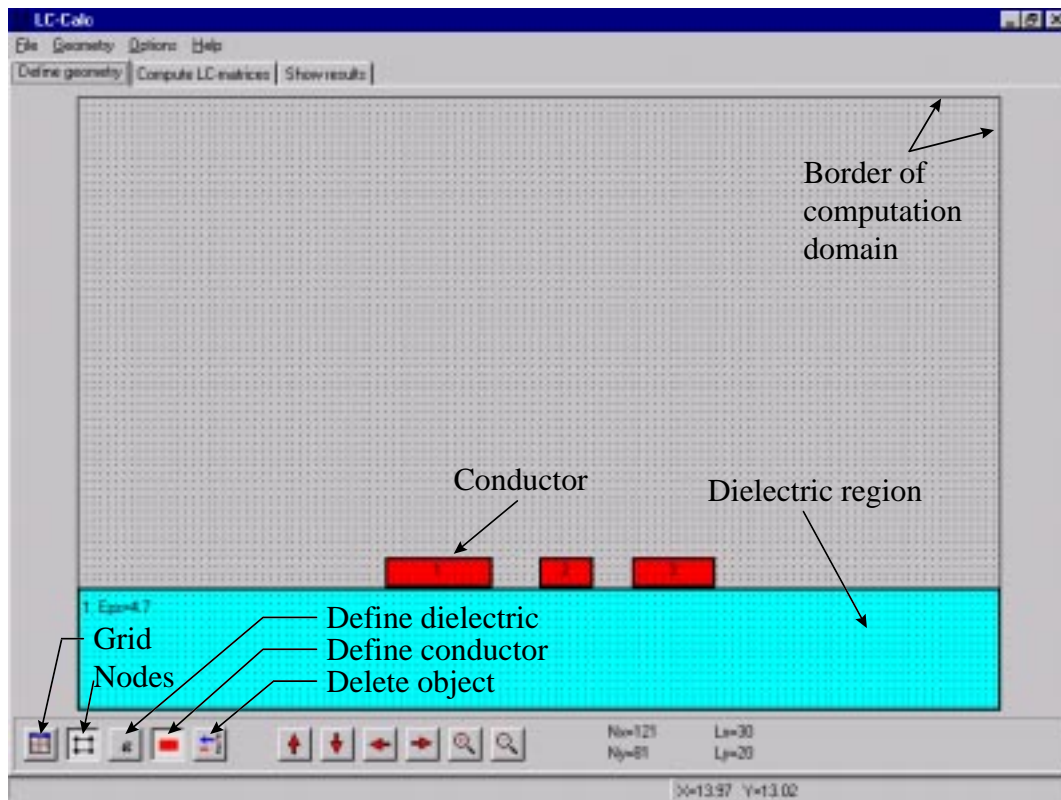


Figure B2. The Define geometry page.

The size of the computation domain and the number of nodes (i.e. the points where the potential is computed) can be changed by clicking the *Grid* button. The size of the computation domain has no dimension so e.g. a length of 10 in the x-direction can mean 10 mm or just as well 10 m, the L- and C-matrices will be the same in both cases. The nodes in the computation domain can be visualised by pressing the *Nodes* button.

A dielectric region within the computation domain is defined by pressing the button marked with an ϵ (Epsilon). A dialog box will appear where the parameters for the region can be set. The dialog box for defining a dielectric region can also be opened from the main menu under Geometry.

Conductors can be added to the geometry by pressing the *Conductor* button. When the button is pressed it will remain down until pressed again. When the mouse is moved over the computation domain the mouse pointer will be a cross marking that a conductor can be defined. By holding down the left mouse button and dragging out a rectangle a conductor is added. The define conductor mode is disabled by clicking on the conductor button again (so it will be in the up state). Conductors can also be defined or edited using dialog boxes that can be opened from the main menu under Geometry.

Dielectric regions or conductors can be deleted by pressing the button with a minus sign (the *Delete* button). A dialog box will appear where which object to be deleted can be selected.

Compute LC-matrices page

This page is used for setting the computation parameters and launch the computation. The computation will determine the L- and C-matrices for the configuration defined on the define geometry page.

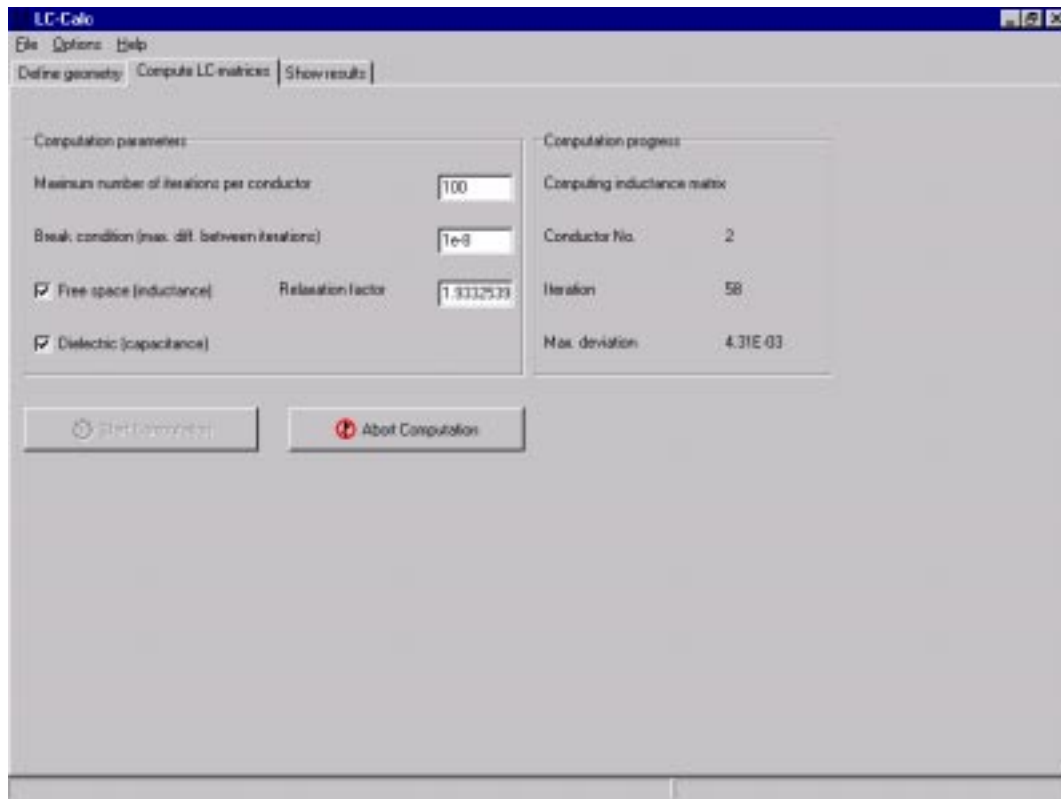


Figure B3. The Compute LC-matrices page.

The solution is found by an iterative procedure as described in Appendix A. There are two parameters that are used for stopping the iterations, the maximum number of iterations and the break condition. The maximum number of iterations and the break condition can be changed by entering a new number in the edit boxes. The break condition is defined as the maximum allowed difference between potential values for two subsequent iterations, i.e. a measure of the convergence of the solution. The smaller value for the break condition (up to a certain point) the better results. The iteration is stopped whenever the criteria for one of the two parameters are met.

The relaxation factor is a constant that is used in order to speed up the convergence of the solution. This factor must be in the interval 1-2 in order for the iteration to converge. Usually the program suggest a value for the relaxation factor based on the size and step size of the computation domain. This suggestion will not be the optimum value for the relaxation factor but will often be quite close to the optimum.

Depending on whether a dielectric region is defined or not one or two computation requests can be marked, free space and dielectric. In order to compute the inductance matrix (even if a dielectric region is defined) the free space choice has to be marked, in this case the capacitance matrix for the free space case will also be computed (i.e. the C-matrix with all dielectric removed). To compute the capacitance matrix when a dielectric region is defined the dielectric choice has to be marked.

The computation is started by pressing the *Start computation* button. When the computation is started information about the progress will be shown on the screen and an abort button will appear. The computation can be stopped before the solution has converged by pressing the *Abort computation* button.

Show results page

When a computation has been performed the L- and C-matrices can be viewed by selecting this page.

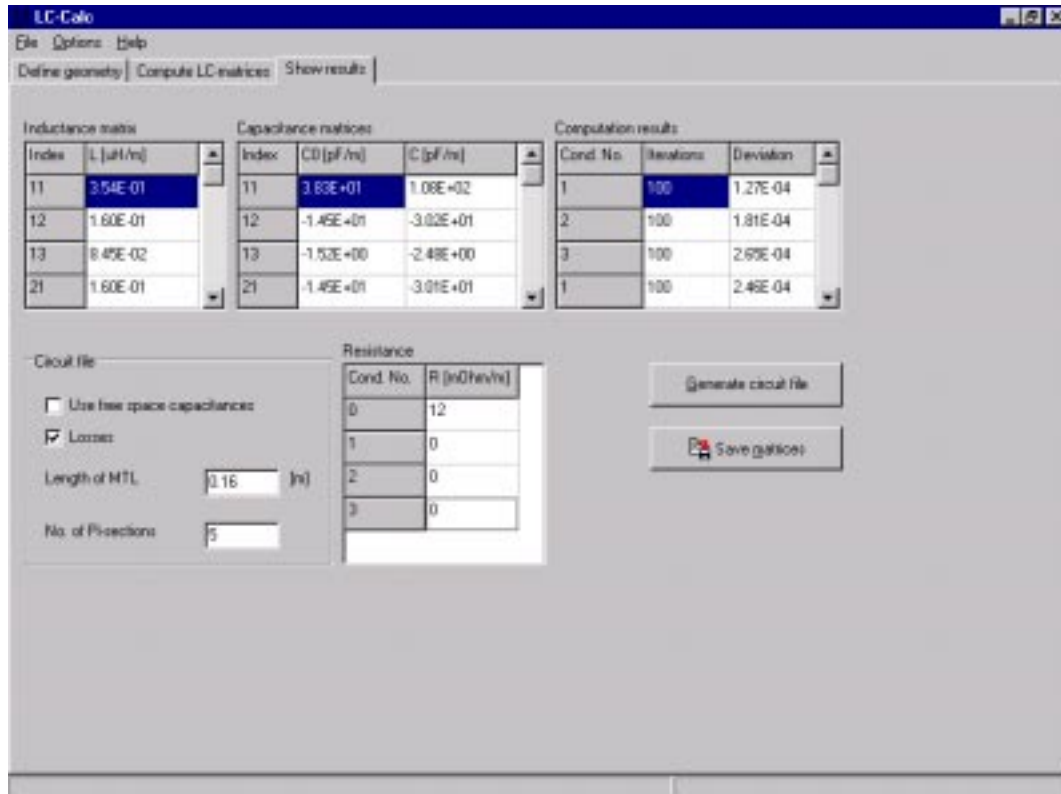


Figure B4. The Show results page.

By pressing the *Generate circuit file* button a SPICE circuit file using the parameters in the circuit file box will be created. The file will be an ASCII-file with the extension CIR.

The computed L- and C-matrices are saved in files when the *Save matrices* button is pressed. These files will have the same name as the project and the following extensions:

- Inductance matrix: IND
- Free space capacitance matrix: COX
- Capacitance matrix taking the dielectrics into account: CDX

File formats

All files generated by LC-Calc are in ASCII format and saved under the project name but with different file extensions. The files are:

*.FDM	File containing information about the computation domain, number of nodes and step sizes
*.PEC	Conductor file containing geometrical data for conductors
*.EPS	Contains data for dielectric regions
*.COX	Free space capacitance matrix
*.CDX	Capacitance matrix when dielectric regions are taken into account
*.IND	Inductance matrix
*.CIR	SPICE circuit file

When the *Save potentials and field distributions* is checked under the *Options* in the main menu the following files are also saved:

*.Fx	Free space potential distribution when conductor x is set to unity, all others are set to zero
*.EFx	Free space electric field distribution when conductor x is set to unity, all others are set to zero
*.Dx	Potential distribution taken dielectric regions into account when conductor x is set to unity, all others are set to zero
*.EDx	Electric field distribution taken dielectric regions into account when conductor x is set to unity, all others are set to zero

The format for the different files are as follows:

*.FDM

Number of nodes in x-direction, Number of nodes in y-direction, Step size in x-direction, Step size in y-direction

*.PEC

Node number in x-direction for left boundary, Node number in x-direction for right boundary, Node number in y-direction for bottom boundary, Node number in y-direction for top boundary

For each conductor data according to above will be added. Note that node number starts with one for nodes at the boundary of the computation domain and counts from left and bottom, respectively.

*.EPS

Node number in y-direction for bottom boundary, Node number in y-direction for top boundary, Relative dielectric constant

For each dielectric region data according to above will be added.

*.COX, *.CDX and *.IND

Row number, Column number, Value

...
...

Where row and column numbers define the position in the corresponding matrix. Values are in either F/m or H/m.

*.CIR

Standard SPICE file where the first comment lines state the node numbers for the input and output of the transmission line.

*.FX and *.DX

Node number in x-direction, Node number in y-direction, Potential value

...
...

*.EFx and *.Edx

Node number in x-direction, Node number in y-direction, E_x value, E_y value

...
...